# The Norfolk Ridge: A Proximal Record of the Tonga-Kermadec Subduction Initiation

J Collot, R Sutherland, S Etienne, M Patriat, W R Roest, B. Marcaillou, C Clerc, W Stratford, N Mortimer, C Juan, et al.

Geochemistry, Geophysics, Geosystems®

AGU ADVANCING EARTH AND SPACE SCIENCE

RESEARCH ARTICLE
10.1029/2022GC010721

# The Norfolk Ridge: A Proximal Record of the Tonga-Kermadec Subduction Initiation

**J. Collot[1], R. Sutherland[2], S. Etienne[1,3], M. Patriat[4], W. R. Roest[4], B. Marcaillou[5], C. Clerc[6], W. Stratford[7], N. Mortimer[7], C. Juan[1], A. Bordenave[1,8], P. Schnurle[4], D. Barker[7], S. Williams[9], S. Wolf[10], and M. Crundwell[7]**

[1]Service Géologique de Nouvelle-Calédonie (New Caledonia Geological Survey), DIMENC, Nouméa, New Caledonia, [2]Victoria University of Wellington, Wellington, New Zealand, [3]Now at GEOTRANSFERT-ADERA, UMR 5805 EPOC, Université de Bordeaux, Bordeaux, France, [4]Université de Brest, CNRS, Ifremer, Geo-Ocean, Plouzané, France, [5]Université Côte d'Azur, IRD, CNRS, Observatoire de la Côte d'Azur, Valbonne, France, [6]Avignon université, UMR 1114 EMMAH, Avignon, France, [7]GNS Science, Lower Hutt, New Zealand, [8]Now at BRGM (French Geological Survey), Geology Division, Orléans, France, [9]State Key Laboratory of Continental Dynamics, Department of Geology, Northwest University, Xían, China, [10]Sorbonne Université, CNRS-INSU, Institut des Sciences de la Terre Paris, ISTeP UMR 7193, Paris, France

**Key Points:**

- We present new marine geophysical and geological data of Norfolk Ridge located along the northeastern edge of the Zealandia continent
- We show that the ridge is not inherited from Cretaceous rifting that led to isolation of Zealandia but from the TECTA Cenozoic tectonic event
- Analysis of the structure and evolution of Norfolk Ridge underpins our understanding of tectonic processes of subduction initiation

**Correspondence to:**
J. Collot,
julien.collot@gouv.nc

**Citation:**
Collot, J., Sutherland, R., Etienne, S., Patriat, M., Roest, W. R., Marcaillou, B., et al. (2023). The Norfolk Ridge: A proximal record of the Tonga-Kermadec subduction initiation. *Geochemistry, Geophysics, Geosystems*, *24*, e2022GC010721. https://doi.org/10.1029/2022GC010721

Received 28 SEP 2022
Accepted 5 FEB 2023

**Author Contributions:**
**Conceptualization:** R. Sutherland, S. Etienne, M. Patriat, W. R. Roest, B. Marcaillou, C. Clerc, W. Stratford, N. Mortimer, C. Juan, A. Bordenave, P. Schnurle, D. Barker, S. Williams, S. Wolf, M. Crundwell
**Investigation:** M. Patriat, W. R. Roest, C. Clerc
**Methodology:** B. Marcaillou
**Software:** B. Marcaillou, C. Juan, P. Schnurle, S. Wolf
**Supervision:** W. R. Roest
**Validation:** R. Sutherland, S. Etienne
**Writing – original draft:** R. Sutherland, S. Etienne, M. Patriat, W. R. Roest, C. Clerc



**Abstract** Norfolk Ridge bounds the northeastern edge of the continent of Zealandia and is proximal to where Cenozoic Tonga-Kermadec subduction initiation occurred. We present and analyze new seismic reflection, bathymetric and rock data from Norfolk Ridge that show it is composed of a thick sedimentary succession and that it was formed and acquired its present-day ridge physiography and architecture during Eocene to Oligocene uplift, emergence and erosion. Contemporaneous subsidence of the adjacent New Caledonia Trough shaped the western slope of Norfolk Ridge and was accompanied by volcanism. Neogene extension along the eastern slope of Norfolk Ridge led to the opening of the Norfolk Basin. Our observations reveal little or no contractional deformation, in contrast to observations elsewhere in Zealandia, and are hence significant for understanding the mechanics of subduction initiation. We suggest that subduction nucleated north of Norfolk Ridge and propagated rapidly along the ridge during the period 40-35 Ma, giving it a linear and narrow shape. Slab roll-back following subduction initiation may have preserved the ridge and created its eastern flank. Our observations suggest that pre-existing structures, which were likely inherited from Cretaceous Gondwana subduction, were well-oriented to propagate rupture and create self-sustaining subduction.

**Plain Language Summary** Plate tectonic theory established and proved that the surface of Earth is composed of rigid moving plates, but it remains unclear how and why these plates sometimes re-configure their boundaries and motions. Subduction zones are places where two plates converge and one plunges deep into the Earth beneath the other one. As the plate sinks, it drags the rest of the plate with it and acts as an engine that "pulls" the plate and drives horizontal motion. This is what drives the dynamics of plate tectonics. How are subduction zones created? This remains an open question, but we know from geological observations that new subduction zones do get created: more than half of all active subduction zones were created after the dinosaurs died out 65 million years ago. We present new observations from northern Zealandia (a submerged continent between New Zealand and New Caledonia) that document how one of the largest subduction zones on Earth, the Tonga-Kermadec system, started.

## 1. Introduction

Subduction zones are the main drivers of plate tectonic motion, but where, when and how subduction initiates remains an open science question and is one of the last great unknowns of plate tectonic theory (Arculus et al., 2019; Cloetingh et al., 1989; Lallemand & Arcay, 2021; Stern & Gerya, 2018). Numerical modeling suggests two end-member competing mechanisms: forced or spontaneous nucleation (Gurnis et al., 2004; Stern, 2004). Spontaneous nucleation occurs when an old cold gravitationally unstable lithosphere next to a younger more buoyant lithosphere sinks under its own weight into the asthenosphere. In that case, models predict subsidence, extension and rift-associated magmatism during initiation (Arculus et al., 2015; Leng & Gurnis, 2015; Stern & Gerya, 2018). Forced nucleation occurs when external factors induce compressional stresses within a plate and force the lithosphere down into the mantle along a zone of preexisting weakness, such as a mid-ocean ridge

**Writing – review & editing:** R. Sutherland, M. Patriat, W. Stratford, N. Mortimer

or a fracture zone (Gurnis et al., 2004; Hall et al., 2003). In that case, models predict a high state of stress and 100–150 km of shortening in order to create a fault, followed by rapid uplift on the hanging wall, the proto-forearc, and subsidence of the footwall in the proto-trench (Gurnis et al., 2004).

Comprehensive geological records of subduction initiation are sparse. Studies from the Izu-Bonin-Mariana (IBM) (Arculus et al., 2015; Leng & Gurnis, 2015) and the Tonga-Kermadec systems (Stratford et al., 2022; Sutherland et al., 2017, 2020) reveal contrasted results and interpretations. Rock records from the Amami Sankaku Basin and from the forearc of the IBM subduction zone reveal that incipient stages of the IBM system were marked by subsidence and seafloor spreading, suggesting that the IBM system initiated spontaneously at ca. 50 Ma (Arculus et al., 2015).

Seismic reflection data and rock samples from northern Zealandia reveal that the initiation of Tonga Kermadec subduction caused compression in the overriding plate after 53–48 Ma that lasted until 37–34 Ma. This is the so-called Tectonic Event of the Tasman Area (TECTA), and suggests induced initiation (Stratford et al., 2022; Sutherland et al., 2017). Based on results from the International Ocean Discovery Program (IODP) Expedition 371, Sutherland et al. (2020) propose that Tonga Kermadec subduction nucleated in the north and a subduction initiation rupture event, which combines spontaneous and dynamically forced mechanisms, propagated southward. Termination of the subduction rupture event at its southern-most extent was associated with widespread TECTA deformation. Deep seismic imaging of the Puysegur subduction zone in the south Tasman Sea, which is currently in a state of forced nucleation, corroborates this idea because it shows that inherited buoyancy contrasts and structural weaknesses play a key role in subduction initiation (Shuck et al., 2021).

The Norfolk Ridge is a continental ribbon at the eastern edge of northern Zealandia (Mortimer et al., 2017). It is located in a key position at the boundary between Neogene volcanic arcs and backarc basins to the east and Paleozoic and Mesozoic basement rocks overlain by Cretaceous-Cenozoic sedimentary basins to the west (Figure 1) (Collot et al., 2009, 2012; Maurizot, Bordenave, et al., 2020; Maurizot, Cluzel, Meffre, et al., 2020; Mortimer, 2004; Sutherland, 1999). The Norfolk Ridge is proximal to where Tonga Kermadec subduction initiation is hypothesized to have taken place and constitutes the margins of the enigmatic New Caledonia and Norfolk basins (DiCaprio et al., 2009; Gurnis et al., 2004; Sutherland et al., 2010, 2017, 2020). Norfolk Ridge is mostly submarine but emerges in New Caledonia, Norfolk Island, and northern New Zealand. The geology of New Caledonia and northern New Zealand is well known (Isaac, 1996; Maurizot and Mortimer, 2020; Rait et al., 1991) and the stratigraphy around the transition zone at the southern end of Norfolk Ridge, Reinga Basin, is well surveyed and was drilled at IODP Site U1508 (Bache et al., 2012; Orr et al., 2020; Stratford et al., 2022; Sutherland et al., 2020). However, because data coverage over Norfolk Ridge is poor, the structure, geology and stratigraphy of the ridge remain undocumented. Studying this ridge offers a unique opportunity to depict subduction initiation processes.

We present new geophysical and geological data from two voyages (TECTA and VESPA) conducted on RV L'Atalante in 2015 (Collot et al., 2016; Patriat et al., 2015). We describe and analyze the Cenozoic stratigraphy and structural style of Norfolk Ridge and discuss implications for understanding the tectonic evolution of the region with respect to subduction initiation processes. This paper is the first comprehensive description of Norfolk Ridge, which is ∼1,500 km long and lies in a key location for understanding the Cenozoic tectonic development of the region.

## 2. Tectonic and Geological Setting

### 2.1. Geodynamics

During the Jurassic to Early Cretaceous time, Zealandia (Figure 1) was located along the eastern convergent margin of the Gondwana super-continent and regions that were to become New Caledonia and northeastern New Zealand were in a forearc position (Cluzel & Meffre, 2002). Widespread continental rifting affected this region during the early Late Cretaceous (∼110–80 Ma) and subsequent Late Cretaceous to early Eocene seafloor spreading of the Tasman Sea (83–52 Ma) isolated Zealandia from Gondwana (Gaina et al., 1998; Hayes & Ringis, 1973).

Relative plate motions can be considered in three main phases (Collot et al., 2020): (a) a period of Tasman Sea opening from 83 to 52 Ma; (b) a transition period from 52 to 43 Ma involving subduction initiation; and (c) a

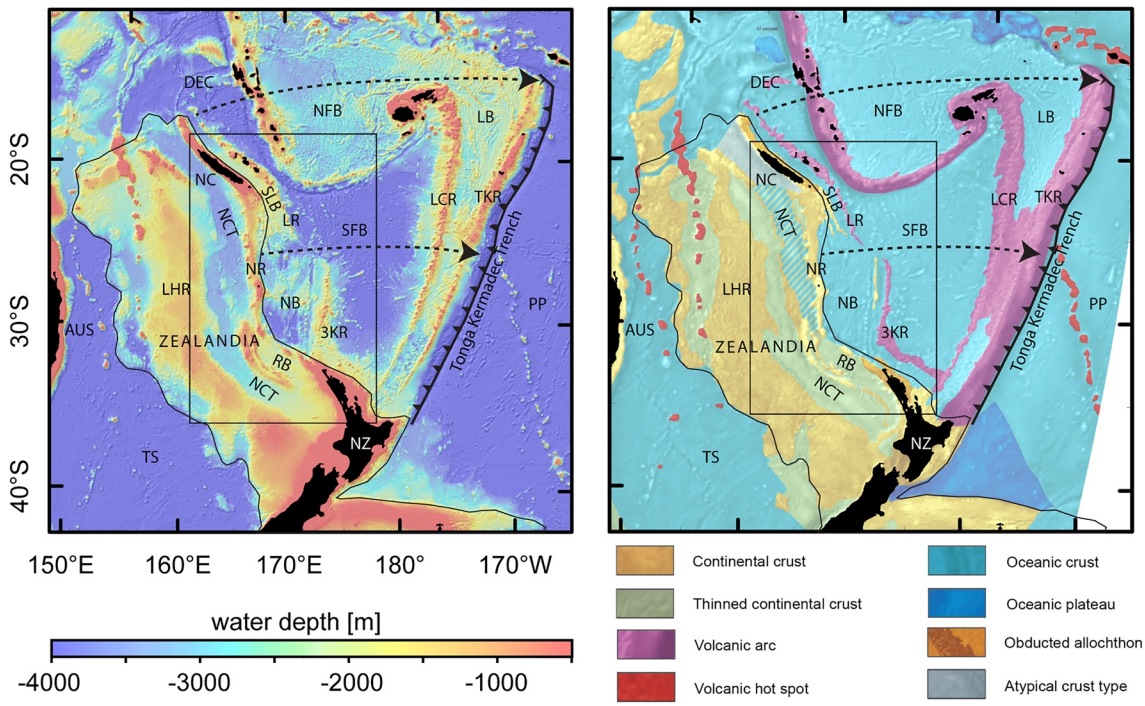


**Figure 1.** The SW Pacific region. (a) Regional bathymetric map. (b) Regional map showing the nature of basement, after Collot et al. (2012). Black line outlines the Zealandia continent. Dashed arrows show the movement (retreat) of the Tonga Kermadec subduction zone, in a schematic fashion (actual backarc basin opening directions are more complex). The black rectangle outlines the location of Figure 2. AUS: Australia, TS: Tasman Sea, LHR: Lord Howe Rise, NC: New Caledonia, NCT: New Caledonia Trough, NR: Norfolk Ridge, RB: Reinga Basin, DEC: D'Entrecasteaux Ridge, NB: Norfolk Basin, LR: Loyalty Ridge, 3KR: Three Kings Ridge, NFB: North Fiji Basin, SFB: South Fiji Basin, LCR: Lau Colville Ridge, LB: Lau Basin, TKR: Tonga Kermadec Ridge, PP: Pacific Plate, NZ: New Zealand.

period after 43 Ma during which Tonga Kermadec subduction evolved into its present state where the Pacific Plate subducts beneath the Australian Plate and retreats eastward. The Tasman Sea opening separated northern Zealandia from Australia, but it remains unclear whether northern Zealandia was part of the Pacific plate before 52 Ma (Steinberger et al., 2004). Southwest Pacific plate closure calculations cannot reliably resolve any motion between northern Zealandia and the Pacific plate during the interval 83-52 Ma, but several authors have proposed the possibility of subduction zones with back-arc basins (with minor net motion) between the Pacific plate and Norfolk Ridge during this time (Cluzel et al., 2001, 2006; Collot et al., 2020; Matthews et al., 2015; Schellart et al., 2006). At ~52 Ma, the Tasman Sea stopped spreading, IBM subduction nucleated, and absolute motion of the Pacific plate started to change, as manifested by the Emperor-Hawaii seamount chain geometry (Arculus et al., 2015; Gaina et al., 1998; O'Connor et al., 2013). By 43 Ma, western Pacific subduction systems were established from Japan to Tonga (Meffre et al., 2012; Reagan et al., 2010), the Emperor-Hawaii bend was complete (O'Connor et al., 2013), and Australia started to move rapidly northwards, away from Antarctica and toward the western Pacific (Cande & Stock, 2004).

Most geological structures located between the Norfolk Ridge and the active subduction systems of Tonga Kermadec and Vanuatu are thought to be younger than 43 Ma (Sdrolias et al., 2003). A few Cretaceous basalts have been dated from the Tonga forearc (Falloon et al., 2014) and Archean to Cretaceous xenocrysts are reported from arc volcanic rocks of the Solomon Islands and Espiritu Santo (Buys et al., 2014; Tapster et al., 2014), but they remain anomalies in what is otherwise a region dominated by arcs and back-arc basins younger than 43 Ma. The oldest arc rocks found in the Tonga forearc are ~45–48 Ma (Bloomer et al., 1995; Duncan et al., 1985; McDougall et al., 1994; Meffre et al., 2012). The Norfolk Basin is located immediately east of Norfolk Ridge and is thought to have opened as the back-arc of westward-dipping and eastward retreating Tonga Kermadec subduction, but the basin may contain hyper-extended continental fragments that were previously contiguous with the Norfolk Ridge (DiCaprio et al., 2009). Three Kings Ridge (Figure 1) is a relic Oligocene to early Miocene arc (Agranier et al., 2023; Gans et al., 2022; Mortimer et al., 1998), and is offset from its northern equivalent, Loyalty Ridge, by the Cook Fracture Zone (Figure 2). Magnetic anomaly and seafloor fabric interpretation combined with the

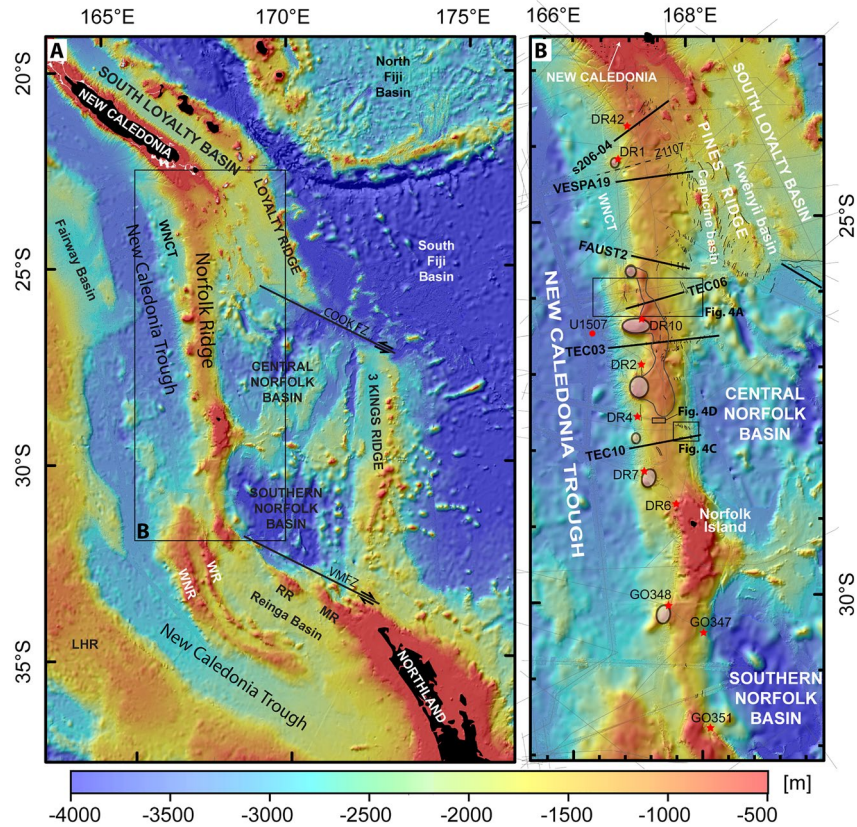


**Figure 2.** (a) Bathymetric map of the area between New Caledonia and Northland New Zealand. (b) Inset location map of Norfolk Ridge. Stars indicate dredge locations. DR1 to DR7 are from the VESPA cruise. DR10 is from SS01/2003. The red circle is the position of the International Ocean Discovery Program site U1507. Bold black lines represent reflection seismic profiles shown in this paper. Dashed line is the position of the wide-angle seismic profile Z1107. LHR: Lord Howe Rise, WNCT: West New Caledonia Basin, WNR: West Norfolk Ridge, WR: Wanganella Ridge, RR: Reinga Ridge, MR: Maria Ridge, VMFZ: Vening Meinesz Fracture Zone. Bathymetric data is a combination of satellite altimetry data (Smith & Sandwell, 1997) and a compilation of shipborne multibeam data (Karthikeyan et al., 2022).

age of dredged rocks show that Cook Fracture Zone activity was synchronous with the opening of the South Fiji and Norfolk basins during the interval 34–15 Ma (Herzer et al., 2011).

It has been suggested on the basis of field observations from New Caledonia that several microplates were active and several subduction flips took place during the interval 70 to 50 Ma (Aitchison et al., 1995; Cluzel et al., 2001; Schellart et al., 2006; Whattam, 2009). In these models, the South Loyalty Basin (Figures 1, Figure 2) opens as a backarc basin to a west-dipping eastward-retreating subduction that flips at ~50 Ma into an east-dipping westward-retreating subduction. Once the South Loyalty Basin was entirely consumed, its margin (Norfolk Ridge) presumably entered the subduction zone and became locked during the Eocene, leading to obduction in New Caledonia. However, no Paleocene or Eocene volcanic arc has been found to support this interpretation. For a review of these geodynamic models, see Collot et al. (2020).

### 2.2. Physiography and Geology of Norfolk Ridge

Norfolk Ridge is oriented north-south, is 1,500 km long and 50–100 km wide. It is connected to Grande Terre, New Caledonia, in the north and to Northland, New Zealand, in the south (Figures 1, Figure 2) (Collot et al., 2009; Eade, 1988; Ravenne et al., 1977). Its crest is typically at 1,000–1,200 m below sea level, except along two shallower terraces: one is located between 26°S and 27.5°S at 500–700 m water depth, and the other is around Norfolk Island at 50–100 m water depth (Figure 2). Quaternary coral reefs and intraplate basalts dated at 2–3 Ma crop out on Norfolk Island (Jones & McDougall, 1973). Seven unnamed seamounts (white ellipses in Figure 2b), ranging from 10 to 40 km in diameter and 1–2 km in height and with tops culminating at 500–100 m water-depth,

are located on the western flank of the ridge (Mortimer et al., 2020). The western slope of Norfolk Ridge deepens toward the New Caledonia Trough (NCT), which reaches 3,500 m water-depth. At the northwestern end of the ridge the West New Caledonia Basin (Figure 2) (Lafoy et al., 2005) is expressed as a 100 km wide, 2,500 m deep terrace that overhangs the NCT. To the east, the ridge is flanked from north to south, by the 2,500 m deep Pines Ridge that marks the offshore continuation of the New Caledonian ophiolite (Auzende et al., 2000; Patriat et al., 2018), the central Norfolk Basin at 3,500 m water-depth, and the southern Norfolk Basin at 5,000 m water depth, respectively.

Dupont et al. (1975) interpreted low-fold seismic reflection profiles and identified a > 3,000 m thick sedimentary cover on Norfolk Ridge, a sedimentary faulted acoustic basement, volcanic intrusions and normal faults that offset sedimentary cover on the flanks of the ridge. They describe Norfolk Ridge as a perched syncline tilted toward the east.

In terms of basement geology, wide-angle seismic refraction profiles shot across the northern ridge sector (see location of profile Z1107 on Figure 2) reveal a 20–25 km thick crust with typical continental crust velocities (Klingelhoefer et al., 2007; Shor et al., 1971). Rocks dredged during research cruises GEORSTOM (Monzier & Vallot, 1983), SS01/2003 (Crawford, 2004) and VESPA (Patriat et al., 2015) are the only offshore samples of the ridge (see location on Figure 2). Dredge GO348 recovered a 26.3 ± 0.1 Ma shoshonite dated by Ar/Ar on biotite and 23–16 Ma shallow-water limestone (Mortimer et al., 1998). Dredge GO347 recovered Late Oligocene to Early Miocene limestones containing shallow-water fossils and rounded lithic and pebbly limestones with bathyal ooze cavity fillings of probable Pliocene to Recent age (Herzer & Mascle, 1996). Dredge GO351 comprises Late Cretaceous black shales, late Eocene siliceous mudstones and middle to late Eocene sedimentary breccias (Herzer & Mascle, 1996). Dredge SS01/2003 DR10 recovered andesitic to trachyandesitic lava, but dating and analytical results have not yet been published (Crawford, 2004). Igneous samples from dredge sites DR1, DR4 and DR7 collected during VESPA along seamounts located on the western flank of the ridge are dated by Ar/Ar on biotite at respectively 31.1 ± 0.6 Ma, 33 ± 5 Ma and 21.5 ± 0.1 Ma (Mortimer et al., 2020). DR1 and DR7 have shoshonitic signatures and DR4 shows affinities with ocean island basalts (Mortimer et al., 2020). DR4 also sampled Late Eocene to Early Oligocene sandy mudstones likely deposited in lower bathyal water-depths (Lawrence et al., 2019) and Middle to Late Eocene bathyal limestones with volcanic breccia (Crundwell et al., 2016). Late Pliocene to early Pleistocene inner shelf calcareous litharenite samples were collected at site VESPA DR6 on the northern slope of the Norfolk Island platform (Lawrence et al., 2019). Samples of late Miocene weakly indurated foram ooze to chalk, likely deposited in mid-bathyal to deeper environments, were recovered at site VESPA DR2. VESPA DR42 targeted a scarp identified on seismic data where deep parts of the stratigraphy of the ridge are emergent at the seafloor (Patriat et al., 2015). This dredge recovered limestones with predominant shallow-water benthic foraminifera of probable Late Oligocene age (Lawrence et al., 2019), hard-ground laminated silicified limestone of undefined age and an Early Miocene lower bathyal calcareous mudstone (Crundwell et al., 2016; Gans et al., 2022). Farther east in the Norfolk Basin, several fossils found within a sandstone and conglomerate, including a fossil leaf, dredged at site SS01/2003 DR28 are interpreted as the relicts of a large latest Eocene to earliest Miocene island (Meffre et al., 2006).

### 2.3. Geology of New Caledonia (Figure 3a)

New Caledonia's main island, called Grande Terre, is the emergent northern end of Norfolk Ridge (Figure 2). Basement geology of Grande Terre is composed of several terranes that formed along the Phanerozoic active margin of Gondwana. The Permian to Late Jurassic Central Chain and Teremba terranes are composed of volcanoclastic arc sediments (Cluzel & Meffre, 2002). The Boghen Terrane is Jurassic high-pressure low-temperature (HP/LT) metamorphic complex composed of sediments, arc-related volcanic rocks and oceanic basalts. The Koh Terrane is a late Carboniferous ophiolite.

Late Cretaceous to Paleocene sedimentary rocks unconformably overlie basement terranes and are associated with rift and post-rift phases. Late Cretaceous syn-rift siliciclastic sediments include coaly sandstones and volcanics (Maurizot, Bordenave, et al., 2020). Paleocene post-rift deep-water biogenic deposits include cherts and calcareous micrites. Eocene shallow-water carbonate platforms (e.g., Uitoé limestone) locally sit directly on the basement, and is overlain by a thick series of clastic, fine to coarse-grained, deep-water basinal turbidites (e.g., Bourail Flysch) that are interpreted to be coeval with southwestward emplacement of several allochthonous Cretaceous to Eocene sedimentary and mafic nappes (e.g., Montagnes Blanches and Poya nappes) (Maurizot,

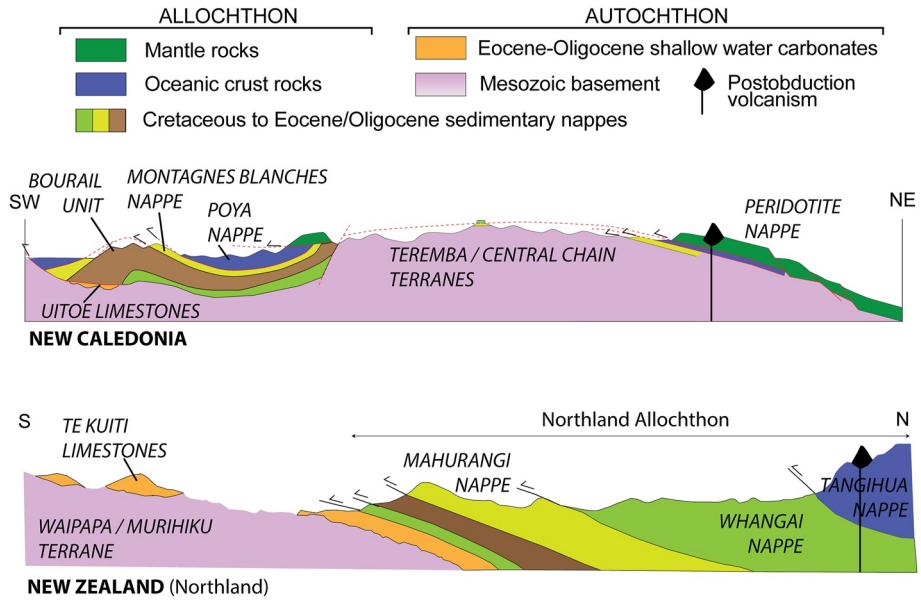


**Figure 3.** New Caledonia and Northland New Zealand synthetic geological cross sections. Modified after (Isaac, 2017; Isaac, Herzer, et al., 1994; Hayward, 2017; Maurizot & Vendé-Leclerc, 2009).

Cluzel, Patriat, et al., 2020). The latest Eocene is marked by obduction of ultramafic sheets (Peridotite Nappe), emplaced toward the southwest, that cap all other geological units except Miocene shallow marine sediments (Maurizot, Cluzel, Patriat, et al., 2020). Post-obduction uplift-related extensional tectonics affects Grande Terre during Neogene (Collot et al., 2017; Lagabrielle et al., 2005; Maurizot et al., 2016; Sevin et al., 2020; Tournadour et al., 2020). Patriat et al. (2018) showed that ultramafic nappes extend offshore to the south for 400 km along Pines Ridge. Oligocene post-obduction granitoids intrude the ophiolite and are interpreted as slab-derived (Cluzel et al., 2005; Paquette & Cluzel, 2007) or post-orogenic (Lagabrielle & Chauvet, 2008).

Eocene metamorphism of Cretaceous and Paleocene sediments and volcanics created blueschists and eclogites (Pouebo Terrane) that are exposed in northern Grande Terre. Pro-grade metamorphism started at 55–50 Ma, based on the ages of detrital zircons and metamorphic mica (Pirard & Spandler, 2017; Vitale Brovarone et al., 2018). Peak metamorphism was at ~44 Ma, and exhumation and cooling took place until ~34 Ma (Baldwin et al., 2007; Spandler et al., 2005).

### 2.4. Geology of Northland New Zealand (Figure 3b)

Northland, New Zealand, is part of the structural southern continuation of the Norfolk Ridge system. At about 31°S the relatively narrow and straight Norfolk Ridge splits and widens into the Reinga Ridge and West Norfolk Ridge, with the Reinga Basin in between them (Figure 2) (Bache et al., 2012; Herzer, 1992, 1995; Herzer et al., 1997, 1999; Orr et al., 2020). Basement rock in Northland is composed of two terranes that were accreted to the Gondwana margin (Isaac, Brook, et al., 1994). The Waipapa Terrane is Permian (Adams & Maas, 2004) to Jurassic in age. It is composed of turbidites and mélange that are interpreted to have formed by the juxtaposition of sedimentary and volcanic slices in a deforming accretionary prism at the Gondwana subduction margin (Spörli et al., 1989). The Murihiku Terrane contains Triassic to Early Cretaceous volcanoclastic deposits of a volcanic forearc basin (Isaac, Herzer, et al., 1994), and is regarded as a Teremba Terrane equivalent. Mesozoic igneous rocks of the Median Batholith have been drilled west of Northland, dredged from West Norfolk Ridge, and inferred beneath the margins of NCT from magnetic anomalies (Mortimer et al., 1997, 1998; Sutherland, 1999).

Late Cretaceous to Paleocene autochthonous sedimentary rocks have little or no exposure in onshore Northland, but are sampled offshore in petroleum wells. Late Cretaceous syn-rift clastic deposits contain coal (e.g., Rakopi Formation) and post-rift Cretaceous and Paleocene marine sediments (e.g., Kapuni Group) similar to those found in New Caledonia (King & Thrasher, 1996). Late Eocene (45–35 Ma) convergence resulted in folding of the northern Reinga Basin and an earlier phase (56–43 Ma) accompanied by adjacent subsidence in the NCT is recognized

**Table 1**
*Characteristics of the Seismic Acquisition Devices*

| Cruise | Streamer length (km) | Number of channels | Receiver immersion (m) | Source volume (cu) | Source immersion (m) | Source band width (Hz) | Shot interval (m) | Seismic processing |
|---|---|---|---|---|---|---|---|---|
| FAUST2 | 0.6 | 6 | 7 | 300 | 10 | 50–130 | 50 | Time migrated |
| VESPA | 0.6 | 24 | 7 | 300 | 7 | 50–130 | 50 | Time migrated |
| TECTA | 4.5 | 720 | 7 | 2,690 | 10 | 7–110 | 50 | Pre-stack time migrated |
| s206 | 3.3 | 264 | 10 | 3,000 | 10 | 50–60 | 50 | Time migrated |

adjacent to the West Norfolk and Wanganella ridges (Bache et al., 2012; Herzer et al., 1997; Orr et al., 2020; Skinner & Sutherland, 2022; Stratford et al., 2022). Similar to New Caledonia, this Eocene convergence is thought to have resulted in local uplift and development of Eocene to Oligocene shelfal to shallow-marine sandstones and limestones (e.g., Tekuiti Group) that rest unconformably on basement rocks (Barrett, 1967; Edbrooke et al., 1998). Allochthonous nappes of Cretaceous to Oligocene sedimentary (e.g., Whangai Nappe, Mahurangi Nappe of the Motatau Complex) and volcanic (e.g., Tangihua Nappe) material was emplaced southwestward in Northland at 23–20 Ma, and a similar nappe (South Maria Allochthon) was emplaced just northwest of Northland (along Maria Ridge, see Figure 2) at 34–28 Ma (Orr et al., 2020). Immediately after allochthon emplacement, the region-experienced arc volcanism (Hayward et al., 2001; Herzer, 1995; Orr et al., 2020).

## 3. Results

Seismic reflection data were acquired during the TECTA and VESPA voyages (Collot et al., 2016; Patriat et al., 2015), and were supplemented by multichannel data from the S206, and FAUST2 voyages (Juan et al., 2015; Lafoy et al., 1998; Mauffret et al., 2002). The TECTA seismic images are pre-stack time-migrated (Juan et al., 2016) and all other profiles are post-stack time-migrated (Sutherland et al., 2012). A classical processing sequence was applied to the data that included common depth point binning, mutes, bandpass filters, spherical divergence correction, source deconvolution, antimultiple, normal move out, automatic gain control, Kirchhoff time migration and stacking. The seismic equipment used and processing techniques are detailed in Table 1. Vertical exaggerations are estimated using seismic velocities of 2,000 m/s and are indicated on all seismic figures as an informative value. A compilation of multibeam bathymetric data (Karthikeyan et al., 2022), that includes new data from these voyages, is also presented and analyzed in this paper.

### 3.1. Seafloor Morphology

The overall seafloor morphology of the Norfolk Ridge is smooth, regular (cf. Section 2.2) and asymmetric, with its western flank being steeper than its eastern flank. Multibeam bathymetric data reveal several key features.

- Linear scarps along the flanks of the ridge are typically 100–200 m high and strike parallel to the ridge axis (Figures 4a–4c).
- Regular seafloor undulations parallel to the ridge axis are interpreted as sediment dunes on the crest of the ridge with wavelengths of 100–400 m and heights of 8–15 m (see Figure 4d).
- Slope gullies and canyons on the western flank of the ridge have lengths between 15 and 50 km, and composite stepped scarps (Figure 4). The size and density of canyons increase around conic edifices. In contrast, no canyons or gullies were observed on the eastern flank of Norfolk Ridge.
- Numerous cone-shaped features with diameters from 100 m to several kilometers and heights from a few hundred meters to 1,500 m are exclusively located near the crest of the western flank of the ridge. They are particularly abundant along the terrace located between 25°S and 27°S (see location of terrace on Figure 2 and detailed morphology on Figures 4a and 4b), and around the six large cone-shaped bathymetric features. Their density can reach one per square-kilometer, although isolated features are also common.

### 3.2. Seismic Reflection Data

#### 3.2.1. General Structure and Seismic Stratigraphy

Using the principles of seismic stratigraphy and analysis of seismic reflection character and unconformities (Mitchum et al., 1977), we define two first order seismic stratigraphic units (NR1 and NR2) that are visible all

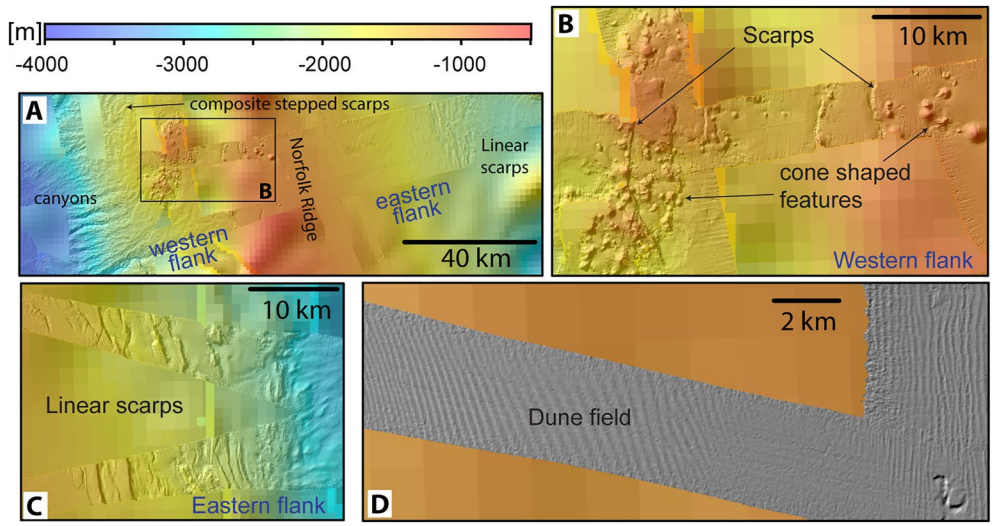


**Figure 4.** Bathymetric insets (see location in Figure 2). (a) East-west bathymetric map of Norfolk Ridge. Note the differences between eastern and western flanks away from volcanoes: the western flank is more abrupt and exhibits canyons and conic edifices, whereas the eastern flank is smoother with linear scarps close to the bottom of the slope. (b) Detailed bathymetry reveals numerous conic edifices around scarps. (c) Linear scarps along the eastern flank. (d) Shaded bathymetry showing dune field around the crest of the ridge. Bathymetric data is a combination of satellite altimetry data (Smith & Sandwell, 1997) and a compilation of shipborne multibeam data (Karthikeyan et al., 2022).

along the ridge, and second order, more local units (NRL1, NRV) that are systematically located between NR1 and NR2. The ridge displays a first-order structural style and stratigraphic pattern that are similar from north to south. Seismic lines FAUST02-76b and TECTA-10 (respectively Figures 5 and 6) illustrate this structure and stratigraphy.

The deepest seismic unit, which we name Norfolk Ridge 1 (NR1), is topped by an unconformity (UNR) and its base is never imaged. Seismic penetration in this unit is typically less than 3 s twt, even with 131 L (8,000 cu in) single bubble source (e.g., Zoneco11-07 seismic profile reported in Klingelhoefer et al., 2007). The unit is

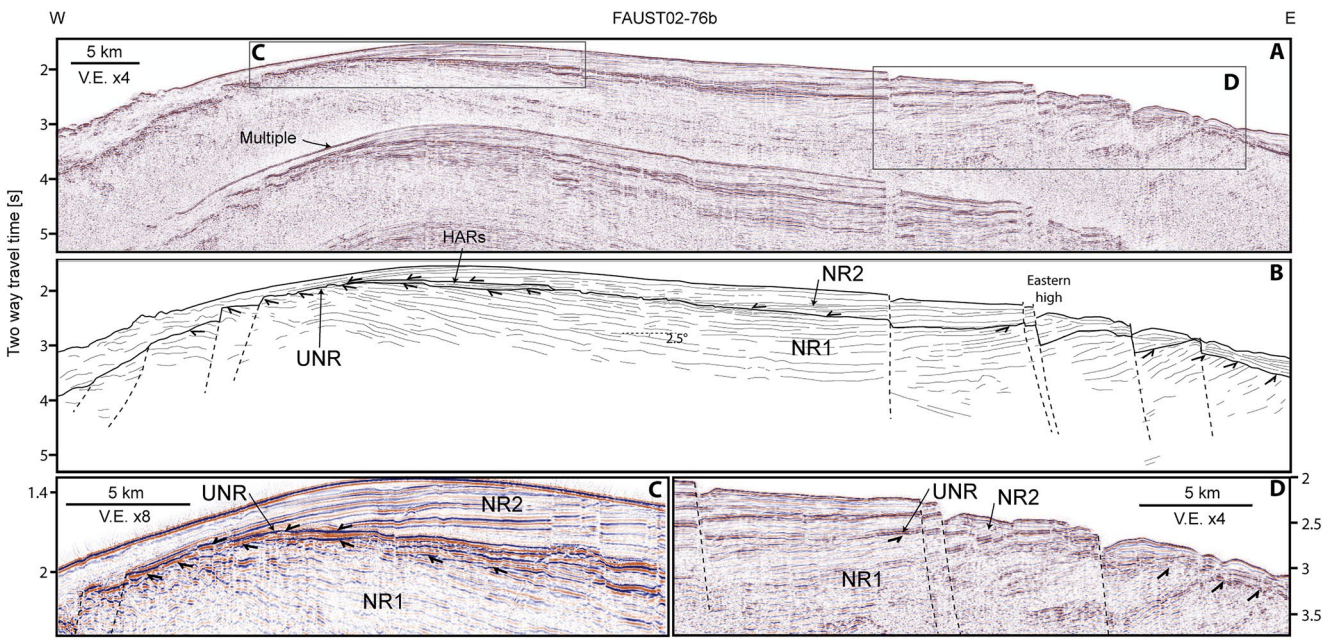


**Figure 5.** Seismic profile FAUST2-076b across Norfolk Ridge. (a) Uninterpreted profile. (b) Interpreted line drawing. (c) Inset showing toplaps beneath unconformity UNR and migrating geometries of NR2 downlapping onto Norfolk Ridge 1 (NR1). (d) Inset showing steep normal faults that offset NR1 and NR2.

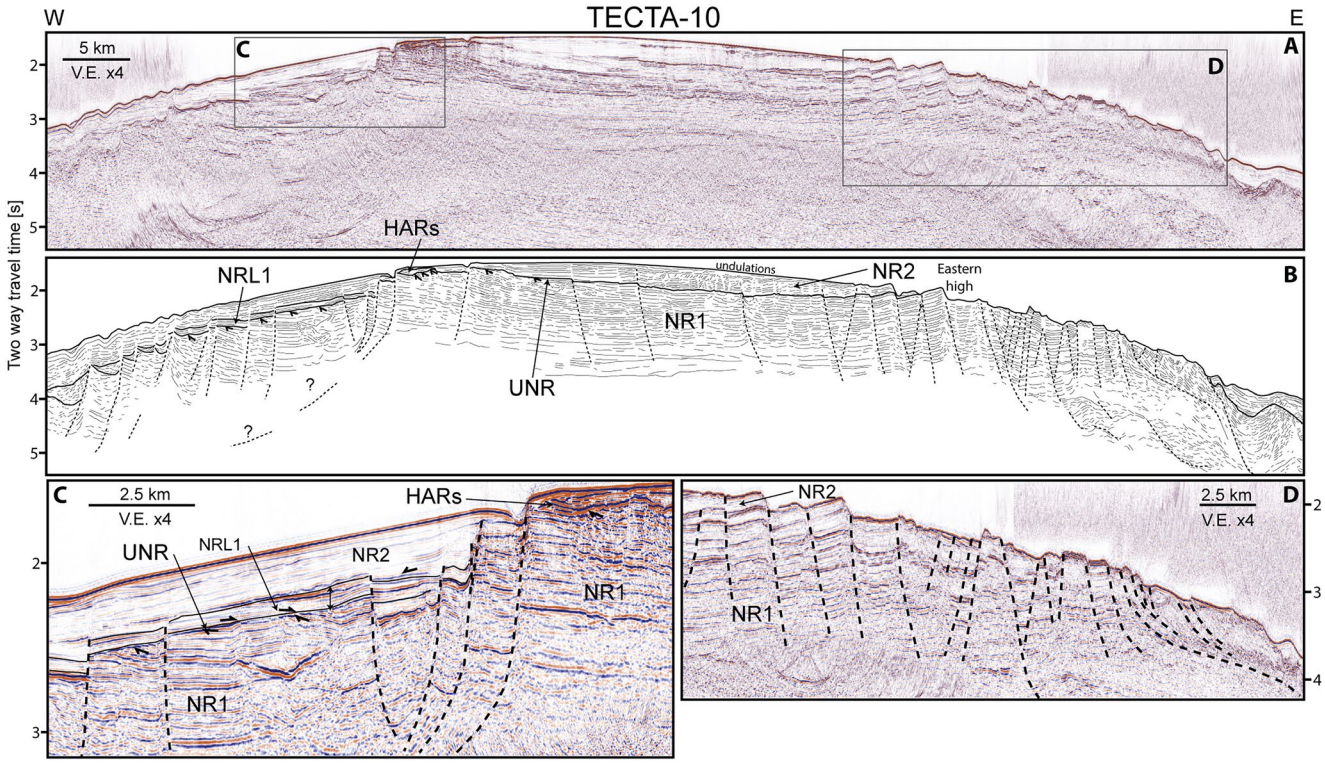


**Figure 6.** Seismic profile TECTA-10. (a) Uninterpreted profile. (b) Interpreted line drawing. (c) Inset showing toplaps beneath UNR and the typical structuration of the western flank of the ridge. Note that normal faults offset UNR and seismic unit NRL1 is deposited on UNR. (d) Inset showing steep normal faults that offset sediments of Norfolk Ridge 1 and NR2.

difficult to image, suggesting low impedance contrasts, but the presence of coherent reflections suggests it is a sedimentary or volcaniclastic unit and that the thickness of NR1 exceeds 2 s twt.

Seismic unit NR1 contains medium to high amplitude, low frequency, and moderate to high continuity reflections. Reflections regionally dip east with a mean slope of 2.5° (e.g., Figures 5 and 6). Beneath the western flank of the ridge, reflections of NR1 are truncated by UNR that marks a prominent angular unconformity (Figures 5 and 6). UNR is flat, tilted toward the west and offset by normal faults that dip westward beneath the west flank (Figure 6c). Locally, (e.g., Figure 6c) a thin (<0.2 s twt) seismic unit (NRL1) overlies UNR and it is also offset by normal faults. NRL1 has high amplitude reflections (HARs) and onlaps UNR.

Along the eastern flank of the ridge, UNR is subparallel and paraconformable with NR1, and it dips eastwards and exhibits an irregular morphology that locally truncates reflections of NR1 (Figures 5 and 6). Locally, at the easternmost extremity of the ridge, UNR is horizontal, or dip westward, to form a topographic high that reaches in some places the same height as the western high (e.g., "Eastern high" on Figures 5–8). This eastern topographic high is systematically crosscut by a series of closely spaced (ca 5–10 km) steep east-dipping normal faults that offset the seafloor and the sedimentary column by >200 m. This fault scarps correspond to the linear bathymetric features that strike parallel to the crest of the ridge and are observed in the multibeam data set (see Section 3.1). Multibeam bathymetric data show that these faults are present all along the ridge (Figure 2). In this position along the eastern flank of the ridge, reflections of NR1 are locally tilted westwards and could be attributed to rotation of blocks of NR1 although no associated low-angle detachments are observed (Figures 5 and 6). UNR is also offset by normal faults, and locally outcrops on the seafloor. A dozen of conjugate cross-cutting normal faults with opposite dipping directions are present along profile TECTA-10 (Figure 6) and could be interpreted as flower-structures.

Seismic unit NR2 is between the seafloor and the top of NR1, except locally where second-order seismic units (e.g., NRL1 and NRV) are present between the two. It is made of high-continuity sub-parallel low-amplitude reflections that cover the ridge unevenly, exposing NR1 on the seafloor in some places. Seismic profile FAUST02-76b (Figure 5) shows the typical stratal pattern of NR2, with migrating geometries onlapping to downlapping

onto NR1. NR2 is thicker on the eastern flank of the ridge. Its top locally displays undulations that correspond to the dunes observed on multibeam bathymetric data (see Section 3.1 and Figure 2). NR2 covers and is not offset by normal faults on the western flank of the ridge (e.g., Figure 6) and, when present, is offset by normal faults on the eastern flank (e.g., Figure 5). NR2 is thicker between the two structural highs formed by the topography of UNR. The western high is created by the eastward dip of NR1 that produces the first-order bathymetric high of the ridge.

Unit NR2 varies in thickness and does not evenly drape the ridge, even in >1 km water depths, and has sediment dunes at its top (Figure 2), and migrating bedform geometries beneath (e.g., Figure 5). This suggests that NR2 is a pelagic unit whose deposition was controlled by deep-water bottom currents that have now likely evolved into the East Australian Current and Tasman Front (Oke et al., 2019; Sutherland et al., 2022). Along the present-day slope break of the western margin, NR2 displays several upslope tilted blocks of reflections that affect the seafloor and correspond to a series of stepped scarps and associated troughs visible on bathymetry (see Figures 4 and 7). The blocks are separated by low-dip or sub-horizontal normal faults that merge along shallow intra-sedimentary detachments that could in some place coincide with UNR (Figure 7). These structures resemble the arcuate ridges described by Etienne et al. (2018) along the western margin of the NCT and are interpreted as the result of unstable unconsolidated calcareous ooze and chalk sliding down-slope.

In the northern part of the ridge and on its western flank (Figure 7), NR2 displays numerous high-amplitude reflections contained within V-shaped erosional features that are interbedded with very low-amplitude continuous reflections. These features can reach 2.5 km in width and 150 ms twt in height and are essentially located within the upper half of the NR2 (Figure 7). The base of these features is marked by a single HAR.

At the crest of the ridge, where the angular unconformity UNR is prominent, HARs are commonly observed between NR1 and NR2, above UNR (e.g., Figures 5, 6, and 8). Rocks dredged at site VESPA-DR42 on seismic profile s206-04 (Figure 8) near the unconformity sampled these HARs and revealed Late Oligocene shallow-water carbonates and hard ground silicified limestone (see Section 2.2).

#### 3.2.2. Volcanics

Seismic images of the terrace located between 26°S and 27.5°S reveal the internal structure of cone-shaped bathymetric features (Figure 9), which we interpret to be of volcanic origin. Seismic line TECTA-06 (Figure 9) shows that one of these volcanic edifices erupted during the deposition of seismic unit NR2 and is laterally connected to a seismic unit we call NRV. NRV is interbedded within NR2, has very HARs, is ca. 20–30 ms twt thick and progressively thins out away from the volcano. Along the terrace, where NRV is prominent, the underlying seismic unit NR1 is poorly imaged. Indeed, reflections of NR1 beneath the eastern flank of Norfolk Ridge progressively become fainter laterally toward the west into bland chaotic basement-like facies (see Figure 9). This could be due to the NRV acting as a screen, preventing seismic energy penetration. Seismic line TECTA-03 (Figure 10) located in the middle of the terrace has a HAR from the seabed, very low seismic penetration, and this profile images only one seismic unit at the summit of the ridge composed of HARs that we attribute to NR1 that are likely masked by a superficial equivalent of NRV. The seismic line also reveals a volcano along the western flank of the ridge that is stratigraphically continuous with a unit that we attribute to NRV with low-continuity high-amplitude internal reflectivity. Of particular note in this area is the fact that NR2 is absent on the top of the ridge and only present on its western flank, overlying the volcano. We attribute this lack of sediments on the ridge to the impact of strong currents at the crest of the terrace. Figure 9 shows an older volcanic edifice that sits on NR1 and is truncated by UNR. Several other volcanic edifices are imaged in this area and are embedded within NR2.

#### 3.2.3. Compressive Features

Minor signs of contractional deformation are observed in the northern part of the ridge. A wedge-shaped imbricated structure, which is approximatively 10 km wide and comprises ramp anticlines that were emplaced top-to-the-west, is observed on line VESPA-19 (Figure 7) in the northeastern part of the ridge (see detailed image in Patriat et al. (2018)). The floor thrust of this structure seems to root into NR1. The imbricated sheets thus involve sediments of NR1, overthrust UNR and a basal part of NR2. It is subsequently sealed by the uppermost part of NR2. This feature is interpreted by Patriat et al. (2018) as a frontal wedge related to the westward emplacement of the Peridotite Nappe south of New Caledonia. Further to the northwest, seismic line s206-04 (Figure 8) shows an asymmetric anticline (dredged at site VESPA-DR42) that is possibly associated with an

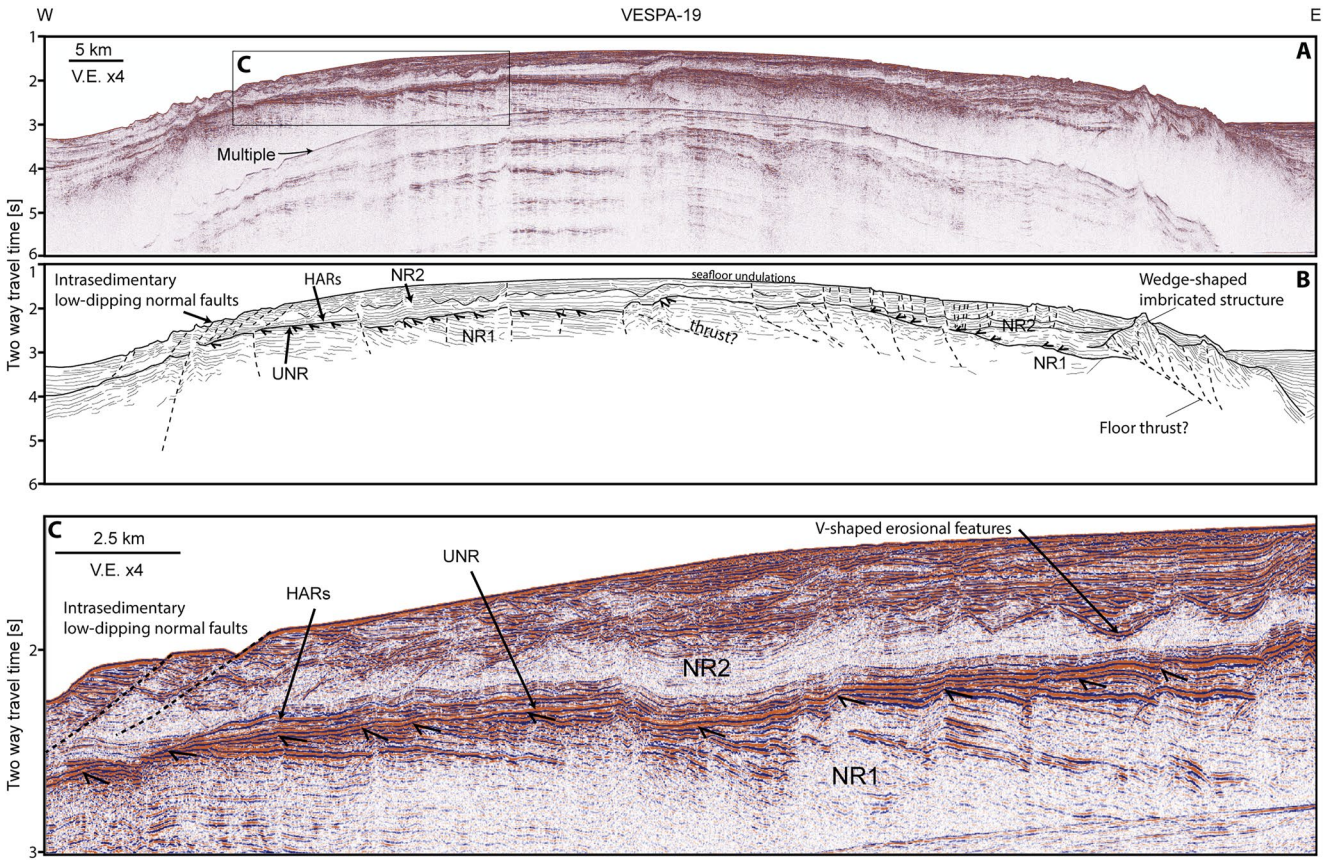


**Figure 7.** Seismic profile VESPA-19 (high resolution). (a) Uninterpreted profile. (b) Interpreted line drawing. (c) Inset showing toplap reflections of Norfolk Ridge 1 beneath UNR, numerous V-shaped erosional features within NR2 interpreted as paleochannels and intrasedimentary low-angle normal faults interpreted as down-slope sliding of NR2.

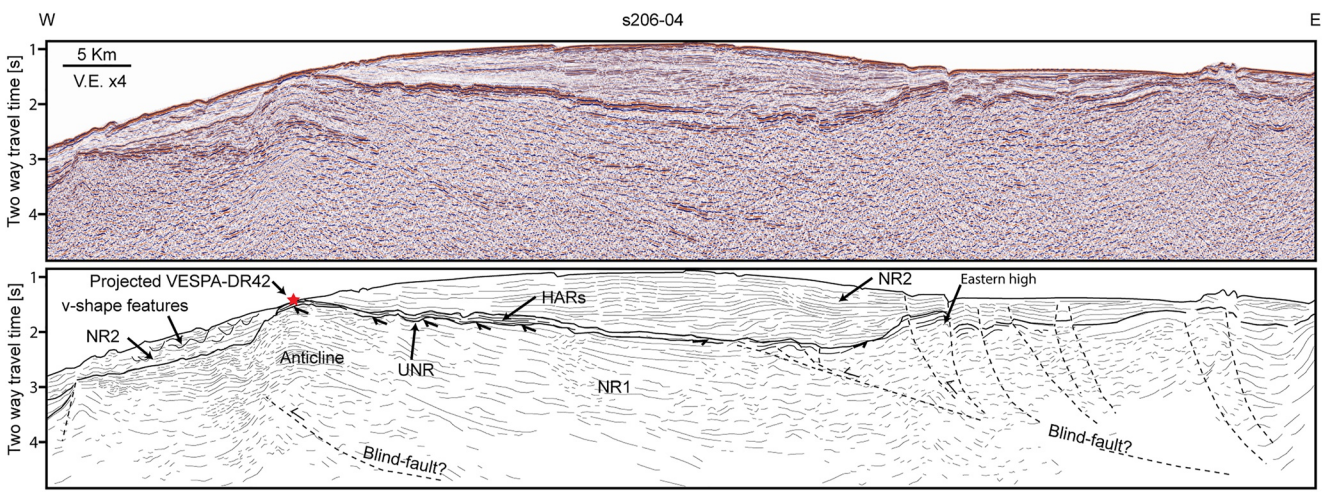


**Figure 8.** Seismic profile s206-04. (a) Uninterpreted profile; (b) interpreted line drawing. VESPA-DR42 dredge site sampled the High Amplitude Reflections at the interface between Norfolk Ridge 1 and NR2 located at the top of an anticline. We interpret the formation of this anticline and the "Eastern High" as the result of deep blind faults.

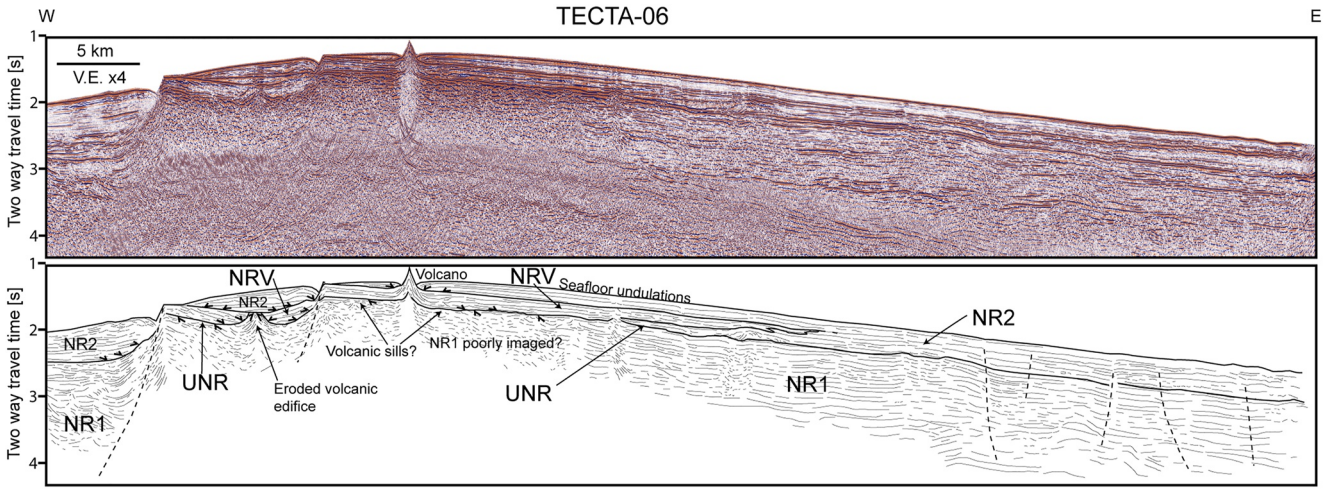


**Figure 9.** Seismic profile TECTA-06. (a) Uninterpreted profile. (b) Interpreted line drawing. Seismic unit NRV is interbedded within NR2 and laterally connected to a volcanic edifice. Norfolk Ridge 1 is poorly imaged along the terrace beneath NRV that could act as a screen and limit penetration of seismic energy.

east-dipping blind thrust fault that deforms sediments of NR1 but is sealed by unit NR2, which is not deformed. This overthrust fold is approximatively 2–3 km wide and >2 s twt thick. Its top crops out on the seafloor and corresponds to UNR, which is marked by HARs. Farther East along this line, NR1 thickens and forms a relief that is approximately 1 s twt high (see "Eastern High" on Figure 8) and is associated with thrust faults.

## 4. Structure and Evolution of Norfolk Ridge

### 4.1. Structure of Norfolk Ridge

The internal structure of Norfolk Ridge returns coherent reflections down to depths that exceed 2–3 s twt beneath the seabed and hence we interpret the ridge geology as being primarily of sedimentary origin (Figures 5–9). Our data do not image crystalline basements, except locally where it is interpreted as volcanic (Figures 9 and 10). Our suggestion that Norfolk Ridge is an ancient Mesozoic to early Cenozoic sedimentary basin or platform that is today perched corroborates the preliminary suggestion of Dupont et al. (1975). A lava dredge at site VESPA-DR1 also contained a small quartz vein xenolith that Mortimer et al. (2020) speculate comes from a schist basement beneath the volcano. The hypothesis is also consistent with the onshore geology of New Caledonia and northern New Zealand, where most exposed pre-Late Cretaceous basement rocks are actually sedimentary in nature (Maurizot, Cluzel, Meffre, et al., 2020; Mortimer, 2004) (pink on Figure 3): Permian to Early Cretaceous

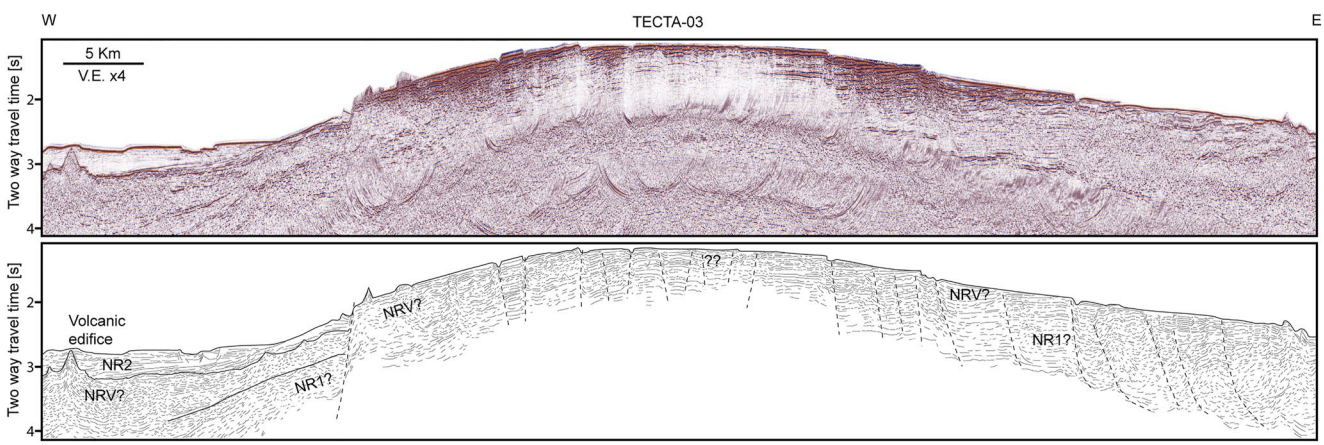


**Figure 10.** Seismic profile TECTA-03 (a) Uninterpreted profile. (b) Interpreted line drawing. This line shows very low seismic penetration and only one seismic unit on the ridge that we attribute to Norfolk Ridge 1. NR2 is absent. This configuration could be due to the action of strong currents (non-deposition or erosion of NR2) or to volcanic activity (superficial volcanic layers preventing seismic energy to penetrate).

sedimentary units, which were deposited or accreted at the Gondwana margin, are overlain by Cretaceous to Eocene syn-rift and post-rift sedimentary cover, then Eocene to Oligocene units represent the emplacement of a series of allochthonous nappes associated with subduction initiation and backarc sedimentary sequences. This interpretation is supported by a few key Late Cretaceous to Eocene deepwater sedimentary rocks sampled along the ridge (see Section 2.2) that record deposition in deep marine environments.

We interpret Oligocene shallow-water calcarenites at the interface between NR1 and NR2 (sampled in dredge VESPA DR42 (Lawrence et al., 2019); location on Figures 2 and 8) as the result of a marine regression-transgression event that recorded uplift and erosion followed by drowning of the UNR truncation surface. Shallow-water fossils could, alternatively, be interpreted as transported from a nearby topographic high, such as from a carbonate platform developed around a volcano, but no such feature is observed upslope of the dredge site VESPA-DR42. High-amplitude reflections from the surface between NR1 and NR2 (HARs in Figures 5–8) are hence interpreted as seismic signatures of a shallow-water cemented carbonate platform. This interpretation is also corroborated by the presence of the hard-ground silicified limestone dredged at site VESPA DR42 (Crundwell et al., 2016). In the northern part of the ridge, we interpret V-shaped erosional features within the basal low-amplitude facies of NR2 as submarine canyons and channels fed by the nearby carbonate platform. At some stage, as the ridge was subsiding, the inferred carbonate platform at the base of NR2 could not keep up with the subsidence, leading to its drowning and to pelagic sedimentation to take over (deposition of NR2). This interpretation is supported by the Early Miocene lower bathyal calcareous mudstone sampled at site VESPA DR42 (Crundwell et al., 2016) that shows that by the Early Miocene the ridge was drowned.

Onshore New Caledonia and Northland, New Zealand, shallow-water carbonates of late Eocene (Uitoé limestones, (Maurizot, 2014; Maurizot, Bordenave, et al., 2020)) and Oligocene (Te Kuiti limestones, (Barrett, 1967; Edbrooke et al., 1998; Isaac, 1996)) age sit unconformably on sedimentary basement terranes of Mesozoic age (respectively Teremba Terrane in NC and Waipapa Terrane in NZ); and contemporaneous calciturbidites in deepwater basins contain detrital products from these carbonate platforms (Bordenave et al., 2021; Maurizot & Cluzel, 2014; Sutherland et al., 2019b, 2019c). Hence, we infer that transient uplift occurred sometime between the Eocene and Oligocene along the entire length of the Norfolk Ridge from New Caledonia to northern New Zealand, though it may be slightly younger in the south.

In New Zealand, the Te Kuiti limestone is overlain by the Northland Allochthon (Hayward et al., 1989; Isaac, Brook, et al., 1994; Jiao et al., 2017). In New Caledonia, the Uitoé limestone is overlain by nappes of Cretaceous to Eocene sedimentary rocks that include syn-tectonic Eocene flysch and post-rift cover (Bordenave, 2019; Espirat, 1989; Maurizot, 2011; Paris, 1977). The development of these shallow-water platforms is interpreted in NC and NZ as recording the drowning of a forebulge associated with progression of the nappes (Bordenave et al., 2021; Maurizot, 2011; Maurizot, Bordenave, et al., 2020). On Norfolk Ridge, nappes are not observed except locally beneath the eastern flank on line VESPA19, where an imbricated wedge that is likely composed of unit NR1 overthrusts the UNR surface toward the west (Figure 7). This wedge is in the same structural position as onshore nappes, which also overthrust an erosional surface on which a transgressive shallow-water carbonate platform deposit exists (i.e., the Uitoé limestones (Maurizot, 2014)).

Our observations lead us to propose that the structure and nature of Norfolk Ridge is similar to that of New Caledonia and northern New Zealand, but nappes of deformed material are rare or not present. We interpret strata of NR1 to be Mesozoic to Paleogene sedimentary rock that is truncated by a shallow-marine or subaerial erosional surface (UNR), which is in turn overlain near the crest of the ridge by an Eocene to Oligocene carbonate platform that rapidly fines upwards into a Neogene calcareous pelagic sequence. A hiatus likely exists between units NR1 and NR2 in most places near the crest of the ridge. Once the ridge drowned, Oligocene to the recent sedimentation was influenced by strong regional currents, such as the East Australian Current and Tasman Front observed today (Oke et al., 2019; Sutherland et al., 2022). This results in large bedforms that unevenly drape the ridge between its various topographic highs to form unit NR2.

The nearby Lord Howe Rise continental ribbon, located 500 km west of Norfolk Ridge, exhibits a regional unconformity, with underlying late Eocene bathyal chalk and overlying Oligo-Miocene carbonate chalks and oozes (Bache et al., 2014; Burns & Andrews, 1973; Stratford et al., 2018; Sutherland et al., 2019a). This unconformity is also observed in the nearby Fairway Basin (Nouzé et al., 2009; Rouillard et al., 2017), NCT (Collot et al., 2008) and Middleton Basin (Boston et al., 2019). The time gap of the hiatus (the age of the unconformity) on Norfolk Ridge (UNR) is not precisely known. However, by comparison with the regional unconformity, the onshore

Eocene-Miocene hiatus in New Caledonia and the sample of shallow-water Oligocene carbonate from the top of UNR, we suggest that the UNR hiatus is between the Eocene and Oligocene.

### 4.2. Formation of Ridge Morphology

Unit NR1 accounts for most of the sediment thickness and there are no clear subdivisions of the unit. Deposition of NR2 was affected by deep-water bottom currents (i.e., heterogeneous thickness, present-day dunes on seafloor, and internal structure suggesting migrating geometries). The contrast in sedimentary styles between units, combined with clear evidence for deformation, uplift, and erosion associated with the formation of the UNR surface, suggests that Norfolk Ridge was a depocenter or platform rather than a topographic high before the tectonic event that formed the erosional surface. This interpretation of Norfolk Ridge being a zone of deposition during NR1 that became inverted to form a topographic high before the deposition of NR2 is corroborated by comparison with the sedimentary filling of the NCT: pre-Oligocene sediments are thinner in the NCT than on Norfolk Ridge whereas post-Eocene sediments are a lot thicker in the basin than on the ridge (see for reference Figure 6 in Sutherland et al. (2010)). Hence, we infer that the present-day first-order physiography of Norfolk Ridge was likely established during a phase of Eocene to Oligocene tectonic inversion. Before that, we interpret Norfolk Ridge as the eastern continental slope of the northern Zealandia continental margin, which has a complex structure inherited from both the Mezosoic active Gondwana margin and Late Cretaceous Zealandia passive margin (see Figure 11).

The inferred change of physiography that created Norfolk Ridge is supported by a drastic change in sedimentation observed at site IODP 371 U1507. This site is located at the base of the western slope of the ridge, in the NCT (see location in Figure 2), where Middle Eocene carbonate pelagic fall out sediments are overlain by Late Eocene to Oligocene high energy turbiditic deposits (Sutherland et al., 2019c, 2020). This confirms that a slope was created along the western flank of Norfolk Ridge during the Eocene to Oligocene and hence that Norfolk Ridge was uplifted at that time. Similar sedimentation regime changes, from a pelagic fall out to calciturbidite reworking, also reflecting slope formation, have been documented in New Caledonia (Dallanave et al., 2018) and New Zealand (Dallanave et al., 2015; Hollis et al., 2005). They are interpreted by Dallanave et al. (2020) as the results of a regional plate motion change that resulted in high rates of plate motion adjacent to northern Zealandia after 46–44 Ma.

The second-order relief formed beneath the easternmost extremity of the ridge at the top of NR1 (UNR) is characteristic of the "perched syncline" structure of Norfolk Ridge (Dupont et al., 1975). The imaged normal faults alone cannot explain the formation of this relief. We suggest that this topography was previously created by thrusting and folding associated with east-dipping blind thrust faults. The numerous normal faults that offset this Eastern High remain sub-vertical and do not merge along east-dipping low-angle detachments. Because of the close spacing of the faults, if these detachments existed, they should be located shallow enough to be imaged on our seismic profiles. This infers that the westward tilt of NR1 strata observed in this location is not the result of block-tilting but rather the result of previous folding. Moreover, these structures are located in the same position as the wedge-shaped imbricated structure observed along the VESPA-19 seismic line (Figure 7 and Patriat al. (2018)).

### 4.3. Normal Faulting

Normal faults parallel to the ridge axis are observed on both margins of the Norfolk Ridge. Both margins have closely spaced faults (ca. 2–3 km spacing), with each system extending over a relatively narrow zone (less than 50 km for the western margin and less than 30 km wide for the eastern margin). Because the faults tend to be closely spaced and have small offsets (and relatively small total heave), they look like normal faults within a broad buldging structure but do not resemble a classic rifted margin configuration in horsts and grabens. The faults accommodated vertical motions associated with the uplift of the Norfolk Ridge and subsidence of the surrounding basins (NCT and Norfolk Basin). Some faults show several hundred meters of vertical throw, but the absence of syn-tectonic fan sedimentation against the fault traces suggests that faulting took place in deep water and there were no local erosional sediment sources or were short-lived.

Eastern and western fault-systems were diachronous. NR2 seals normal faults of the western margin but is offset by normal faults of the eastern margin, implying that western fault activity preceded that of the eastern faults.

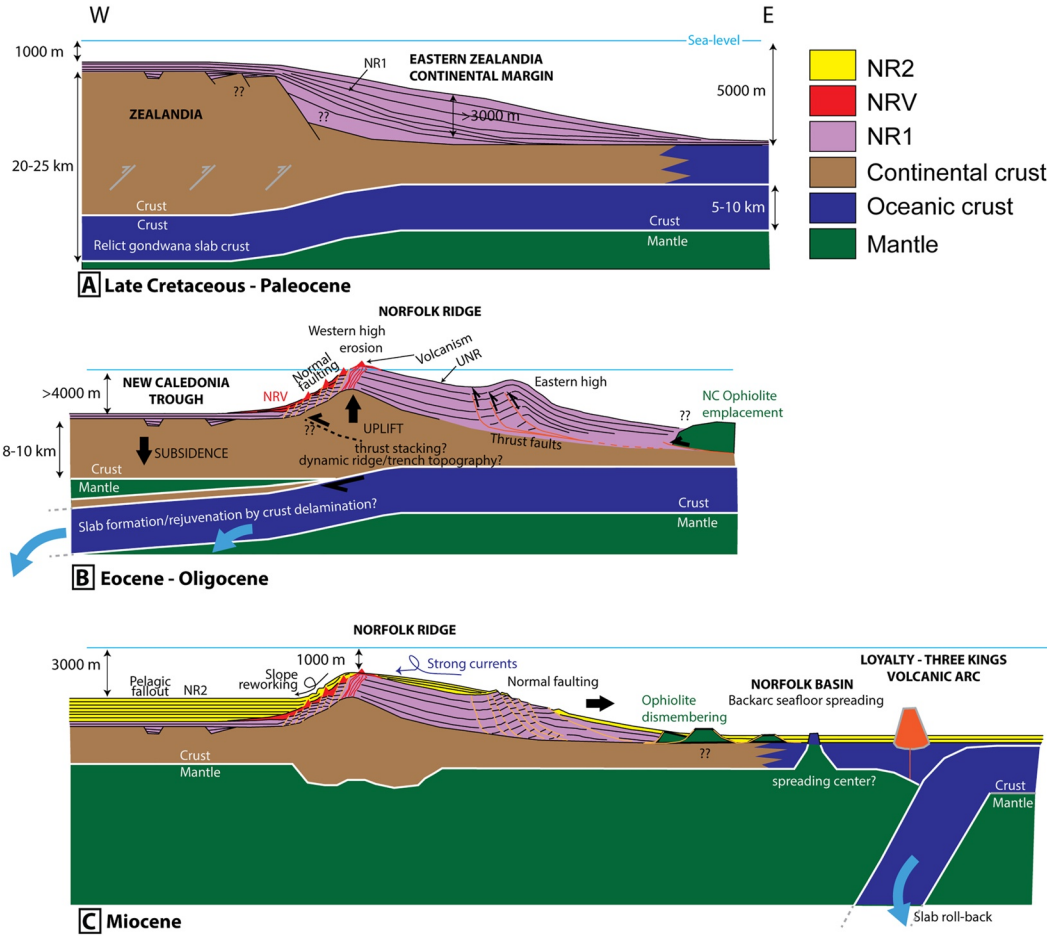


**Figure 11.** Conceptual tectonic model of subduction initiation and formation of Norfolk Ridge. (a) The initial stage is Zealandia's eastern passive continental margin, which has relict subduction structures from the Jurassic to Early Cretaceous Gondwana active margin (schematized as gray faults). (b) Thrust stacking and/or dynamic ridge/trench topography caused the uplift of the Norfolk Ridge, and slab formation or rejuvenation of the relict Gondwana slab by removal of buoyant material in the lower crust through a process of delamination caused the New Caledonia Trough to subside. The combination of these opposite vertical motions led to the formation of Norfolk Ridge during the Eocene to Oligocene. Normal faulting along this narrow area accommodated the differential motion. Volcanism related to deep slab formation and mantle disturbance occurred exclusively at the newly formed basin-ridge boundary. Farther East, the Eastern High forms at this time and is likely related to the frontal thrust of the obducted mantle peridotite allochthon that is known to occur immediately east of Norfolk Ridge. (c) As the slab rolls back, the extension in the overriding plate affects the eastern part of the ridge during the Miocene and leads to backarc opening of the Norfolk Basin and arc volcanism at Loyalty-Three Kings Ridge.

UNR is offset by faults along both margins, indicating that the faults were active after erosion and during subsidence in deep water. This is consistent with the good preservation of fault scarps.

The ages of NR1, NR2, and UNR are inferred from the stratigraphy of the NCT and volcanic dredges. Faulting (with a possible early reverse faulting phase) along the western margin likely occurred during the Eocene to Oligocene and faulting along the eastern margin likely occurred during the Mio-Pliocene. Normal faulting along the western margin is likely associated with formation of the NCT (Baur et al., 2014; Collot et al., 2017; Hackney et al., 2012; Lafoy et al., 2005; Skinner & Sutherland, 2022; Sutherland et al., 2010, 2020) and to uplift of the ridge itself. Normal faulting of the eastern margin is likely associated with the formation of the Norfolk Basin during the Miocene which could include a strike-slip component as indicated by the possible flower structures observed along profile TECTA-10 (Figure 6) (DiCaprio et al., 2009; Herzer et al., 2011; Mortimer et al., 2007). Onshore New Caledonia, postobduction extensional tectonics occurred during the Miocene (Chardon & Chevillotte, 2006; Chevillotte et al., 2006; Lagabrielle et al., 2005).

### 4.4. Volcanism

Cenozoic volcanic activity was concentrated along the western flank of Norfolk Ridge near its crest. There is a prominent N-S alignment of large volcanoes around Norfolk Island and near the deep-water terrace located between latitudes 25.5° and 27.5°S; but smaller volcanic structures, sills and volcaniclastic sedimentary units (c.f. seismic unit NRV) are also present. Volcanic features cluster near normal faults of the western margin of the ridge.

Based on geochemistry and geochronology data, Mortimer et al. (2020) show that the large volcanic chain is not a hotspot track or a volcanic arc, that the ages of individual volcanos spread between late Eocene and early Miocene, and that their atypical origin could either be due to melting near the lithosphere-asthenosphere transition and/or could involve flux melting related to dewatering of a subducted slab. In the NCT, the late Eocene change in sedimentation regime (see Section 4.2) recorded at site IODP 371 U1507 at 36 Ma was accompanied by the onset of the deposition of volcanoclastic breccias (Sutherland et al., 2019c), thus also confirming the temporal relationship between vertical motions, tectonics and volcanism, at least locally. The source of the 36 Ma volcanic clasts from the breccias has been interpreted as the major upslope guyot volcano at latitude −36.5deg labeled DR10 in Figure 2b (Mortimer et al., 2020). Assuming this to be correct, the DR10 volcano is late Eocene to early Oligocene. We propose that sporadic and moderately voluminous Eocene to Miocene volcanism was related to episodic mantle melting linked to the tectonics of formation of the Norfolk Ridge as a physiographic feature (perched sedimentary basin). These include the Eocene-Oligocene tectonic event that generated the vertical motions between the Norfolk Ridge and the NCT associated with normal faulting along the western flank of the ridge.

## 5. Geodynamic Interpretation of Norfolk Ridge

The Norfolk Ridge is the eastern continental margin of the northern Zealandia continent. An erosional unconformity UNR separates seismic stratigraphic units NR1 and NR2, and it is recognized in many places along the Norfolk Ridge. We infer that the unconformity formed during the late-Eocene (after ∼36 Ma) to late Oligocene, based on one dredge sample, IODP drilling at two sites (U1507, U1508) near the ridge flank (Stratford et al., 2022), and clear analogies to the geology of New Caledonia and New Zealand. This Eocene-Oligocene tectonic event was temporally associated with the initiation of subduction that evolved into the Tonga-Kermadec system and/or the related start of backarc basin opening, and it overprinted a more complex Mesozoic tectonic history. We have no direct age control on the thick sedimentary unit NR1 that lies beneath the unconformity.

Direct and compelling evidence for contractional deformation of unit NR1 (or equivalents to the north or south) is restricted to the northern (folds on Figures 7 and 8, this paper) and southern (Bache et al., 2012; Stratford et al., 2022) terminations of the main north-south section of Norfolk Ridge. This is consistent with Eocene deformation in New Caledonia (Bordenave et al., 2021; Maurizot, Bordenave, et al., 2020; Maurizot, Cluzel, Patriat, et al., 2020), and regional observations of TECTA deformation farther west, which are mostly south of the main section of Norfolk Ridge (Stratford et al., 2022; Sutherland et al., 2017), and in Reinga Basin (Orr et al., 2020). Convergent plate motion during the interval 45-25 Ma was substantial (>1,000 km) in the vicinity of Norfolk Ridge (Bache et al., 2012; Gurnis et al., 2004). Although there is no direct evidence of major contractional deformation along the north-south section of Norfolk Ridge, it is still a possibility that our data do not image deep thrusts or that the contractional deformation was overprinted by extensional deformation (e.g., the Eastern High; Figure 8). The uplift that led to erosion associated with UNR and the presence of the second-order topographic relief along the ridge's easternmost flank (Eastern High) suggests that low strain contractional deformation could have affected the entire length of Norfolk Ridge. We also observe many normal faults on Norfolk Ridge with a relatively small offset, and an age progression that goes from older than NR2 in the west, to contemporaneous to NR2 in the east.

We speculate that activity on a fossil subduction thrust beneath Norfolk Ridge (inherited from Gondwana subduction), accommodated all plate convergence during the late Eocene and Oligocene. As Paleogene subduction initiation became established, slab roll-back and trench-retreat rapidly led to extension, volcanism, and backarc basin formation east of Norfolk Ridge during the late Oligocene to Miocene. Slab formation or rejuvenation of a relict Gondwana slab through a process of lower crust delamination beneath the NCT, dynamic ridge-trench topography (Gurnis et al., 2004) and/or crustal thickening of Norfolk Ridge by thrust stacking would have occurred

early in this process. We infer that these were the mechanisms of (a) initial uplift of Norfolk Ridge to form UNR (dynamic ridge/trench topography and/or thickening of the buoyant part of the crust), (b) subsidence of NCT to form the western slope of Norfolk Ridge (removal of buoyant material in the deep crust (Hackney et al., 2012; Sutherland et al., 2010, 2020)), and (c) associated volcanism (Figure 11).

Ophiolite emplacement just east of northern Norfolk Ridge, as described by Patriat et al. (2018), also likely affected the structure of the ridge and could be at the origin of the regional eastward tilt of the ridge through a loading/flexure process and of the formation of the Eastern High as a consequence of the frontal thrust. The mechanisms that relate the emplacement of this supra-subduction ophiolite to subduction initiation beneath Norfolk Ridge remain unclear. There could have been another subduction boundary located farther east, as suggested by Aitchison et al. (1995) and Whattam (2005), but understanding the relationships between these two putative boundaries is beyond the scope of this paper. After roll-back of the slab, crustal underplating may have occurred to thicken the crust and form a persistent ridge (Figure 11), but it was not manifest as widespread folding and thrust faulting in the upper crust. Such an underplating mechanism is inferred to be active today at the Kermadec-Hikurangi subduction margin, which is the active equivalent of the same system (Bassett et al., 2010).

Norfolk Basin is inferred to have formed as a backarc basin during the period 28-16 Ma (Herzer et al., 2011), which is consistent with our inference for the age of UNR and age of normal faulting along the eastern flank of the ridge, and is also consistent with rifting of West Norfolk Ridge (at the southern end of our study area) during the Oligocene (Orr et al., 2020). During this phase, we suggest that the ophiolite was dismembered by extensive normal faulting (Figure 11), leading to the horst and graben structures described by Patriat et al. (2018) north of the Cook Fracture Zone and to the formation of hyper-extended blocks, south of the Cook Fracture Zone within the Norfolk Basin. These blocks could correspond to the crustal fragments described by DiCaprio et al. (2009) and Meffre et al. (2006) in the Norfolk Basin. The Oligocene age of volcanic activity is consistent with it being subduction-related, but if it was caused by reactivation and roll-back of a slab that was already subducted and partially dehydrated in the Cretaceous, that may help to explain the atypical magma chemistry (Mortimer et al., 2020).

## 6. Subduction Initiation Processes

Most authors agree that the initiation of subduction that grew into the Tonga-Kermadec system occurred close to Norfolk Ridge during the Eocene-Oligocene (see (Collot et al., 2020) for review). The lack of convergent deformation and presence of normal faulting along the main north-striking 1,500 km section of Norfolk Ridge is significant. In terms of the classic induced versus spontaneous end member models for subduction initiation (Gurnis et al., 2004; Stern, 2004), this lack of compressive deformation is evidence for spontaneous subduction initiation.

However, this observed deformation style contrasts with that on northwest-striking ridge segments at either end of Norfolk Ridge: Reinga, Maria and West Norfolk Ridges in the south, and the New Caledonia to D'Entrecasteaux section in the north (Figure 2), where evidence for high degrees of convergent deformation (allochthon emplacement in New Caledonia and New Zealand) might be interpreted as evidence for induced subduction initiation.

Sutherland et al. (2020) speculate that, based on the diachronicity of regional uplift-subsidence patterns, a subduction rupture event propagated from north to south during the period 55-20 Ma. We speculate that northwest-striking sections of proto-subduction thrust (e.g., in New Caledonia) had much slower rupture propagation rates than the main north-striking section (Norfolk Ridge), which was more optimally primed for failure, rapid propagation, quickly localized deformation and produced a tensional horizontal stress state. The inference of rapid late Eocene to early Oligocene subduction initiation along the Norfolk Ridge is backed up by the timing of the succession of events at the scale of northern Zealandia. Indeed, the compressional events in the area south of Norfolk Ridge (e.g., Reinga Basin, southern NCT) are dated between 40 and 30 Ma (Bache et al., 2012; Etienne et al., 2018; Orr et al., 2020; Stratford et al., 2022; Sutherland et al., 2017) which overlaps with timing of compressional events in New Caledonia that are dated 45-35 Ma (Bordenave et al., 2021; Collot et al., 2008; Dallanave et al., 2020; Maurizot, Bordenave, et al., 2020). In contrast, the earliest signs of subduction initiation in New Caledonia are dated around 55 Ma (Cluzel et al., 2006, 2012, 2016) and it was not until 24–20 Ma that subduction initiated beneath the northern tip of New Zealand (Herzer, 1995; Rait, 2000; Rait et al., 1991). Together, this suggests that a high degree of convergence could have occurred from 55 to 40 Ma in the area north

of Norfolk Ridge that would have led to subduction nucleation, rapid rupture propagation along Norfolk Ridge from 40 to 35 Ma and slow propagation to Northland between 35 and 25 Ma. The age of opening of adjacent back arc basins shows a similar southward-younging (Herzer et al., 2011) and supports this fundamentally diachronous aspect of SW Pacific tectonics.

## 7. Conclusions

Analysis of newly acquired seismic, bathymetric and rock data combined with known onshore exposures of the Norfolk Ridge reveals for the first time the structure of the Norfolk Ridge and allows us to interpret its evolution. Before the Eocene, Norfolk Ridge was a depocenter along the eastern margin of Zealandia. The present ridge physiography was acquired during the late Eocene to Oligocene.

The formation of the relatively steep western flank of the ridge was the result of focused differential vertical motion between the ridge (uplift) and NCT (subsidence). This phase led to submarine or/and subaerial erosion of the summit of the ridge, over its entire length. Intense late Eocene to Miocene volcanism was located along the western flank of the ridge and accompanied this phase. Signs of early contractional deformation during the ridge formation are sparse but exist at the northern and southern ends. Extensional tectonics affected the entire length of the ridge, with a clear age diachronism. Normal faulting occurred first on the west flank and then on the east.

We interpret the formation and evolution of Norfolk Ridge as surface manifestations of deep lithospheric processes related to Tonga Kermadec subduction initiation along the Zealandia continental margin. Our observations of little or no compressive deformation along Norfolk Ridge, widespread normal faulting, and approximately synchronous time of events along strike (rapid lateral propagation of subduction) are consistent with a spontaneous mode of subduction initiation. This is the opposite conclusion to what was drawn from previous studies at either end of this ridge (New Caledonia to the North and Reinga Basin to the South (Bache et al., 2012; Cluzel et al., 2012; Gurnis et al., 2004; Orr et al., 2020; Sutherland et al., 2017)). The notably different behaviors indicate that the Norfolk Ridge segment of the subduction zone initiated more easily and quickly than adjacent sections.

Additional work is required to sample strata above and below the UNR unconformity on a transect from north to south. Precise dating of this unconformity would allow direct determination of the rate of subduction rupture propagation. Determining the nature of unit NR1 would allow a better understanding of the subsidence history of NCT, as well as the uplift history of Norfolk Ridge. This is significant because both features are inferred to have formed during the process of subduction initiation. Precise paleobathymetry and age models from within unit NR1 would provide a better understanding of the rate and magnitude of subsidence of the ridge crest as the subducted slab retreated and evolved into a mature subduction zone. New data are also required to link the formation of Norfolk Ridge to geological events that occurred farther east, notably the formation and obduction of the New Caledonian ophiolite (Secchiari et al., 2018; Ulrich et al., 2010), the high temperature subduction initiation metamorphic sole (Agard et al., 2018; Cluzel et al., 2012), as well as the burial and exhumation of the high pressure/low temperature metamorphic complex (Baldwin et al., 2007; Spandler & Hermann, 2006; Vitale Brovarone et al., 2018).

Even though there is much still to be discovered in this remote region, our description of the structure and stratigraphy of Norfolk Ridge provides a firm basis for testing models of subduction rupture propagation.

## Data Availability Statement

Multibeam bathymetric grids are available online (https://doi.org/10.12770/38a24abd-9f5a-4108-bb86-a0add3c45d9d and https://www.ausseabed.gov.au/data/bathymetry). Seismic data are available online (https://doi.org/10.17882/92632).

**Acknowledgments**
We thank the Genavir captains and crew of RV L'Atalante during the TECTA (https://doi.org/10.17600/15001300) and VESPA (https://doi.org/10.17600/15001100) voyages conducted in 2015. These two voyages were funded by the Commission Nationale Flotte Hauturière of the French Ministry of Research and Higher Education. Seismic data were processed with the kind support of Université Côte d'Azur and Geovation academic license. We acknowledge the Government of New Caledonia and its Service Géologique de Nouvelle Calédonie, the New Zealand geological survey (GNS-Science), the New Zealand Ministry of Business, Innovation and Employment and l'Institut National des Sciences de l'Univers, CNRS- Institut des Sciences de la Terre, for post-cruise financial support. This work was funded in the framework of the scientific agreement between the Government of New Caledonia and IFREMER. Special thanks goes to Mike Isaac who led with passion the post-cruise field trip in Northland, New Zealand.

## References

Adams, C. J., & Maas, R. (2004). Age/isotopic characterization of the Waipapa group in Northland and Auckland, New Zealand, and implications for the status of the Waipapa terrane. *New Zealand Journal of Geology and Geophysics*, *47*(2), 173–187. https://doi.org/10.1080/00288306.2004.9515046

Agard, P., Plunder, A., Angiboust, S., Bonnet, G., & Ruh, J. (2018). The subduction plate interface: Rock record and mechanical coupling (from long to short timescales). *Lithos*, *320–321*, 537–566. https://doi.org/10.1016/j.lithos.2018.09.029

Agranier, A., Patriat, M., Mortimer, N., Collot, J., Etienne, S., Durance, P., & Gans, P. (2023). Oligo-Miocene subduction-related volcanism of the Loyalty and three Kings Ridges, SW Pacific: A precursor to the Tonga-Kermadec arc. *Lithos*, *436–437*, 436106981. https://doi.org/10.1016/j.lithos.2022.106981

Aitchison, J., Clarke, G., Meffre, S., & Cluzel, D. (1995). Eocene arc-continent collision in New Caledonia and implications for regional southwest Pacific tectonic evolution. *Geology*, *23*(2), 161–164. https://doi.org/10.1130/0091-7613(1995)023<0161:eaccin>2.3.co;2

Arculus, R. J., Gurnis, M., Ishizuka, O., Reagan, M. K., Pearce, J. A., & Sutherland, R. (2019). How to create new subduction zones. *Oceanography*, *32*(1), 160–174. https://doi.org/10.5670/oceanog.2019.140

Arculus, R. J., Ishizuka, O., Bogus, K. A., Gurnis, M., Hickey-Vargas, R., Aljahdali, M. H., et al. (2015). A record of spontaneous subduction initiation in the Izu–Bonin–Mariana arc. *Nature Geoscience*, *8*(9), 728–733. https://doi.org/10.1038/ngeo2515

Auzende, J. M., Van de Beuque, S., Regnier, M., Lafoy, Y., & Symonds, P. (2000). Origin of the New Caledonian ophiolites based on a French-Australian seismic transect. *Marine Geology*, *162*(2–4), 225–236. https://doi.org/10.1016/s0025-3227(99)00082-1

Bache, F., Mortimer, N., Sutherland, R., Collot, J., Rouillard, P., Stagpoole, V., & Nicol, A. (2014). Seismic stratigraphic record of transition from Mesozoic subduction to continental breakup in the Zealandia sector of eastern Gondwana. *Gondwana Research*, *26*(3), 1060–1078. https://doi.org/10.1016/j.gr.2013.08.012

Bache, F., Sutherland, R., Stagpoole, V., Herzer, R. H., Collot, J., & Rouillard, P. (2012). Stratigraphy of the southern Norfolk Ridge and the Reinga Basin: A record of initiation of Tonga–Kermadec–Northland subduction in the southwest Pacific. *Earth and Planetary Science Letters*, *321–322*, 41–53. https://doi.org/10.1016/j.epsl.2011.12.041

Baldwin, S. L., Rawling, T., & Fitzgerald, P. G. (2007). *Thermochronology of the New Caledonian high-pressure terrane: Implications for middle Tertiary plate boundary processes in the southwest Pacific* (Vol. 419, pp. 117–134). Geological Society of America Special Paper.

Barrett, P. J. (1967). Te Kuiti group in the Waitomo-Te Anga area. *New Zealand Journal of Geology and Geophysics*, *10*(4), 1009–1026. https://doi.org/10.1080/00288306.1967.10423204

Bassett, D., Sutherland, R., Henrys, S., Stern, T., Scherwath, M., Benson, A., et al. (2010). Three-dimensional velocity structure of the northern Hikurangi margin, Raukumara, New Zealand: Implications for the growth of continental crust by subduction erosion and tectonic underplating. *Geochemistry, Geophysics, Geosystems*, *11*(10), Q10013. https://doi.org/10.1029/2010gc003137

Baur, J., Sutherland, R., & Stern, T. (2014). Anomalous passive subsidence of deep-water sedimentary basins: A prearc basin example, southern New Caledonia Trough and Taranaki basin, New Zealand. *Basin Research*, *26*(2), 242–268. https://doi.org/10.1111/bre.12030

Bloomer, S. H., Taylor, B., MacLeod, C. J., Stern, R. J., Fryer, P., Hawkins, J. W., & Johnson, L. (1995). Early arc volcanism and the ophiolite problem: A perspective from drilling in the western Pacific. In B. Taylor & J. H. Natland (Eds.), *Active margins and marginal basins of the western Pacific* (Vol. 88, pp. 1–30). American Geophysical Union Monograph.

Bordenave, A. (2019). *Evolution tectono-sédimentaire d'une marge continentale passive en regime d'obduction: l'exemple de la Nouvelle-Calédonie et de son domaine offshore (Sud-Ouest Pacifique), Thèse de doctorat* (p. 376). ENSEGID / Service Géologique de Nouvelle-Calédonie.

Bordenave, A., Etienne, S., Collot, J., Razin, P., Patriat, M., Grélaud, C., et al. (2021). Upper Cretaceous to Palaeogene successions of the Gouaro anticline: Deepwater sedimentary records of the tectonic events that led to obduction in New Caledonia (SW Pacific). *Sedimentary Geology*, *415*, 105818. https://doi.org/10.1016/j.sedgeo.2020.105818

Boston, B., Nakamura, Y., Gallais, F., Hackney, R., Fujie, G., Kodaira, S., et al. (2019). Delayed subsidence after rifting and a record of breakup for northwestern Zealandia. *Journal of Geophysical Research: Solid Earth*, *124*(3), 3057–3072. https://doi.org/10.1029/2018JB016799

Burns, R. E., & Andrews, J. E. (1973). Regional aspects of deep sea drilling in the southwest Pacific. In R. E. Burns, J. E. Andrews, G. J. van der Lingen, M. Churkin, J. S. Galehouse, G. Packham, et al. (Eds.), *Initial reports of the deep sea drilling project* (Vol. 21, pp. 897–906). U.S. Government Printing Office.

Buys, J., Spandler, C., Holm, R. J., & Richards, S. W. (2014). Remnants of ancient Australia in Vanuatu: Implications for crustal evolution in island arcs and tectonic development of the southwest Pacific. *Geology*, *42*(11), 939–942. https://doi.org/10.1130/g36155.1

Cande, S. C., & Stock, J. (2004). Pacific-Antarctic-Australia motion and the formation of the Macquarie Plate. *Geophysical Journal Letters*, *157*(1), 399–414. https://doi.org/10.1111/j.1365-246x.2004.02224.x

Chardon, D., & Chevillotte, V. (2006). Morphotectonic evolution of the New Caledonia ridge (Pacific Southwest) from post-obduction tectono-sedimentary record. *Tectonophysics*, *420*(3–4), 473–491. https://doi.org/10.1016/j.tecto.2006.04.004

Chevillotte, V., Chardon, D., Beauvais, A., Maurizot, P., & Colin, F. (2006). Long term tropical morphogenesis of New Caledonia (Pacific SW): Importance of positive epeirogeny and climate change. *Geomorphology*, *81*(3–4), 361–375. https://doi.org/10.1016/j.geomorph.2006.04.020

Cloetingh, S., Wortel, R., & Vlaar, N. J. (1989). On the initiation of subduction zones. *Subduction Zones Part II*, 7–25. https://doi.org/10.1007/978-3-0348-9140-0_2

Cluzel, D., Aitchison, J. C., & Picard, C. (2001). Tectonic accretion and underplating of mafic terranes in the late Eocene intraoceanic fore-arc of New Caledonia (southwest Pacific): Geodynamic implications. *Tectonophysics*, *340*(1/2), 23–59. https://doi.org/10.1016/s0040-1951(01)00148-2

Cluzel, D., Bosch, D., Paquette, J. L., Lemennicier, Y., Montjoie, P., & Menot, R. P. (2005). Late Oligocene post-obduction granitoids of New Caledonia: A case for reactivated subduction and slab break-off. *Island Arc*, *14*(3), 254–271. https://doi.org/10.1111/j.1440-1738.2005.00470.x

Cluzel, D., Jourdan, F., Meffre, S., Maurizot, P., & Lesimple, S. (2012). The metamorphic sole of New Caledonia ophiolite:40Ar/39Ar, U-Pb, and geochemical evidence for subduction inception at a spreading ridge. *Tectonics*, *31*(3), TC3016. https://doi.org/10.1029/2011tc003085

Cluzel, D., & Meffre, S. (2002). L'unité de la Bohgen (Nouvelle-Calédonie, Pacifique sud-ouest): Un complexe d'accrétion jurassique. Données radiochronologiques préliminaires U-Pb sur les zircons détritiques. *Comptes Rendus Geoscience*, *334*(11), 867–874. https://doi.org/10.1016/s1631-0713(02)01823-0

Cluzel, D., Meffre, S., Maurizot, P., & Crawford, A. J. (2006). Earliest Eocene (53 Ma) convergence in the southwest Pacific: Evidence from pre-obduction dikes in the ophiolite of New Caledonia. *Terra Nova*, *18*(6), 395–402. https://doi.org/10.1111/j.1365-3121.2006.00704.x

Cluzel, D., Ulrich, M., Jourdan, F., Meffre, S., Paquette, J.-L., Audet, M.-A., et al. (2016). Early Eocene clinoenstatite boninite and boninite-series dikes of the ophiolite of New Caledonia; a witness of slab-derived enrichment of the mantle wedge in a nascent volcanic arc. *Lithos*, *260*, 429–442. https://doi.org/10.1016/j.lithos.2016.04.031

Collot, J., Geli, L., Lafoy, Y., Vially, R., Cluzel, D., Klingelhoefer, F., & Nouzé, H. (2008). Tectonic history of northern New Caledonia Basin from deep offshore seismic reflection: Relation to late Eocene obduction in New Caledonia, southwest Pacific. *Tectonics*, *27*(TC6006), 1–20. https://doi.org/10.1029/2008TC002263

Collot, J., Herzer, R. H., Lafoy, Y., & Géli, L. (2009). Mesozoic history of the Fairway—Aotea basin: Implications regarding the early stages of Gondwana fragmentation. *Geochemistry, Geophysics, Geosystems*, *10*(12), Q12019. https://doi.org/10.1029/2009GC002612

Collot, J., Patriat, M., Etienne, S., Rouillard, P., Soetaert, F., Juan, C., et al. (2017). Deepwater fold-and-thrust belt along New Caledonia's western margin: Relation to post-obduction vertical motions. *Tectonics*, *36*(10), 2108–2122. https://doi.org/10.1002/2017TC004542

Collot, J., Patriat, M., Sutherland, R., Williams, S., Cluzel, D., Seton, M., et al. (2020). Geodynamics of the southwest Pacific: A brief review and relations to New Caledonian geology. *New Caledonia - Geology, Geodynamic Evolution, and Mineral Resources*, *51*(1), 13–26. https://doi.org/10.1144/M51-2018-5

Collot, J., Sutherland, R., Roest, W., Patriat, M., Etienne, S., Juan, C., et al. (2016). TECTA voyage report, RV L'Atalante (Vol. *1*, p. 85). Text *Rapport SGNC-2016(01)*. https://doi.org/10.17600/15001300

Collot, J., Vende-Leclerc, M., Rouillard, P., Lafoy, Y., & Géli, L. (2012). Map helps unravel complexities of the Southwestern Pacific Ocean. *Eos Transactions of American Geophysical Union*, *93*(1), 1–2. https://doi.org/10.1029/2012EO010001

Crawford, A. J. (2004). Voyage summary southern surveyor 01/2003, unpublished CSIRO report, updates 22/04/04. Retrieved from https://www.marine.csiro.au/data/reporting/get_file.cfm?eov_pub_id=866%20on%20July%2030%202022

Crundwell, M., Morgans, H. E. G., & Hollis, C. (2016). Micropaleontological report on dredge samples collected during the 2015 VESPA expedition. *GNS Science Internal Report*, 83.

Dallanave, E., Agnini, C., Bachtadse, V., Muttoni, G., Crampton, J. S., Strong, C. P., et al. (2015). Early to middle Eocene magneto-biochronology of the southwest Pacific Ocean and climate influence on sedimentation: Insights from the Mead Stream section, New Zealand. *GSA Bulletin*, *127*(5–6), 643–660. https://doi.org/10.1130/b31147.1

Dallanave, E., Agnini, C., Pascher, K. M., Maurizot, P., Bachtadse, V., Hollis, C. J., et al. (2018). Magneto-biostratigraphic constraints of the Eocene micrite–calciturbidite transition in New Caledonia: Tectonic implications. *New Zealand Journal of Geology and Geophysics*, *61*(2), 145–163. https://doi.org/10.1080/00288306.2018.1443946

Dallanave, E., Maurizot, P., Agnini, C., Sutherland, R., Hollis, C., Collot, J., et al. (2020). Eocene (46-44 Ma) onset of Australia-Pacific plate motion in the southwest Pacific inferred from stratigraphy in New Caledonia and New Zealand. *Geochemistry, Geophysics, Geosystems*, *21*(7), e2019GC008699. https://doi.org/10.1029/2019GC008699

DiCaprio, L., Muller, R. D., Gurnis, M., & Goncharov, A. (2009). Linking active margin dynamics to overriding plate deformation: Synthesizing geophysical images with geological data from the Norfolk Basin. *Geochemistry, Geophysics, Geosystems*, *10*(1), Q01004. https://doi.org/10.1029/2008gc002222

Duncan, R. A., Vallier, T. L., & Falvey, D. A. (1985). *Volcanic episode at 'Eua, Tonga Islands*. Circum-Pacific Council Energy Mineral Resource Earth Science Series.

Dupont, J., Launay, J., Ravenne, C., & De Broin, C. E. (1975). Données nouvelles sur la ride de Norfolk (Sud Ouest Pacifique). *Comptes Rendus de l'Académie des Sciences, Série D*, *281*, 605–608.

Eade, J. V. (1988). The Norfolk Ridge system and its margins. In A. E. M. Nairn, F. G. Stehli, & S. Uyeda (Eds.), *The Ocean basin and margins* (7th ed., pp. 303–324). Plenum Press.

Edbrooke, S. W., Crouch, E. M., Morgans, H. E. G., & Sykes, R. (1998). Late Eocene-Oligocene Te Kuiti group at mount Roskill, Auckland, New Zealand. *New Zealand Journal of Geology and Geophysics*, *41*(1), 85–93. https://doi.org/10.1080/00288306.1998.9514792

Espirat, J. J. (1989). *Carte Géologique à l'échelle du 1/50 000 et notice explicative: Feuille Bourail*. Territoire de la Nouvelle-Calédonie - Bureau de Recherches Géologiques et Minières.

Etienne, S., Collot, J., Sutherland, R., Patriat, M., Bache, F., Rouillard, P., et al. (2018). Deepwater sedimentation and cenozoic deformation in the southern New Caledonia trough (northern Zealandia, SW Pacific). *Marine and Petroleum Geology*, *92*, 764–779. https://doi.org/10.1016/j.marpetgeo.2017.12.007

Falloon, T. J., Meffre, S., Crawford, A. J., Hoernle, K., Hauff, F., Bloomer, S. H., & Wright, D. J. (2014). Cretaceous fore-arc basalts from the Tonga arc: Geochemistry and implications for the tectonic history of the SW Pacific. *Tectonophysics*, *630*, 21–32. https://doi.org/10.1016/j.tecto.2014.05.007

Gaina, C., Mueller, D. R., Royer, J.-Y., Stock, J., Hardebeck, J. L., & Symonds, P. (1998). The tectonic history of the Tasman Sea: A puzzle with 13 pieces. *Journal of Geophysical Research*, *103*(6), 12413–412433. https://doi.org/10.1029/98jb00386

Gans, P. B., Mortimer, N., Patriat, M., Turnbull, R. E., Crundwell, M. P., Agranier, A., et al. (2022). Detailed 40Ar/39Ar geochronology of the Loyalty and Three Kings Ridges clarifies the extent and sequential development of Eocene to Miocene southwest Pacific remnant volcanic arcs. *Geochemistry, Geophysics, Geosystems*, *24*(2), e2022GC010670. https://doi.org/10.1029/2022GC010670

Gurnis, M., Hall, C. E., & Lavier, L. L. (2004). Evolving force balance during incipient subduction. *Geochemistry, Geophysics, Geosystems*, *5*(7), Q07001. https://doi.org/10.01029/02003GC000681

Hackney, R., Sutherland, R., & Collot, J. (2012). Rifting and subduction initiation history of the New Caledonia Trough, southwest Pacific, constrained by process-oriented gravity models. *Geophysical Journal International*, *189*(3), 1293–1305. https://doi.org/10.1111/j.1365-246X.2012.05441.x

Hall, C. E., Gurnis, M., Sdrolias, M., Lavier, L. L., & Mueller, R. D. (2003). Catastrophic initiation of subduction following forced convergence across fracture zones. *Earth and Planetary Science Letters*, *212*(1–2), 15–30. https://doi.org/10.1016/s0012-821x(03)00242-5

Hayes, D. E., & Ringis, J. (1973). Seafloor spreading in the Tasman Sea. *Nature (London)*, *244*(5408), 454–458. https://doi.org/10.1038/243454a0

Hayward, B. W. (2017). *Out of the ocean into the fire. History in the rocks, fossils and landforms of Auckland, Northland and Coromandel* (Vol. 146, p. 336). Geoscience Society of New Zealand Miscellaneous Publication.

Hayward, B. W., Black, P. M., Smith, I. E. M., Ballance, P. F., Itaya, T., Doi, M., et al. (2001). K-Ar ages of early Miocene arc-type volcanoes in northern New Zealand. *New Zealand Journal of Geology and Geophysics*, *44*(2), 285–311. https://doi.org/10.1080/00288306.2001.9514939

Hayward, B. W., Brook, F. J., & Isaac, M. J. (1989). Cretaceous to middle Tertiary stratigraphy, paleogeography and tectonic history of Northland, New Zealand. *Geology of Northland; accretion, allochthons and arcs at the edge of the New Zealand micro-continent* (Vol. 26, pp. 47–64). Royal Society of New Zealand Bulletin.

Herzer, R. H. (1992). The Northland Basin, New Zealand, from rift to active margin; tectonic evolution and petroleum potential. *AAPG Bulletin*, *76*(7), 1107.

Herzer, R. H. (1995). Seismic stratigraphy of a buried volcanic arc, Northland, New Zealand and implications for Neogene subduction. *Marine and Petroleum Geology*, *12*(5), 511–531. https://doi.org/10.1016/0264-8172(95)91506-k

Herzer, R. H., Barker, D., Roest, W., & Mortimer, N. (2011). Oligocene-Miocene spreading history of the northern South Fiji Basin and implications of the New Zealand plate boundary. *Geochemistry, Geophysics, Geosystems*, *12*(2), Q02004. https://doi.org/10.1029/2010gc003291

Herzer, R. H., Chaproniere, G. C. H., Edwards, A. R., Hollis, C. J., Pelletier, B., Raine, J. I., et al. (1997). Seismic stratigraphy and structural history of the Reinga Basin and its margins southern Norfolk Ridge system. *New Zealand Journal of Geology and Geophysics*, *40*(4), 425–451. https://doi.org/10.1080/00288306.1997.9514774

Herzer, R. H., & Mascle, J. (1996). Anatomy of a continent-backarc transform; the Vening Meinesz fracture zone northwest of New Zealand. *Marine Geophysical Researches*, *18*(2/4), 401–427. https://doi.org/10.1007/bf00286087

Herzer, R. H., Sykes, R., Killops, S. D., Funnell, R. H., Burggraf, D. R., Townend, J., et al. (1999). Cretaceous carbonaceous rocks from the Norfolk Ridge system, Southwest Pacific; implications for regional petroleum potential. *New Zealand Journal of Geology and Geophysics*, *42*(1), 57–73. https://doi.org/10.1080/00288306.1999.9514831

Hollis, C. J., Dickens, G. R., Field, B. D., Jones, C. M., & Percy Strong, C. (2005). The Paleocene–Eocene transition at Mead Stream, New Zealand: A southern Pacific record of early cenozoic global change. *Palaeogeography, Palaeoclimatology, Palaeoecology*, *215*(3), 313–343. https://doi.org/10.1016/j.palaeo.2004.09.011

Isaac, M. J. (1996). *Geology of the Kaitaia area: Scale 1:250,000*. Institute of Geological & Nuclear Sciences, Lower Hutt.

Isaac, M. J. (2017). Northland field trip guide, *TECTA-VESPA Southwest Pacific marine geology workshop*.

Isaac, M. J., Brook, F. J., Hayward, B. W., & Herzer, R. H. (1994). *Emplacement of the Northland Allochthon; Recent advances in New Zealand Earth science; abstracts from a seminar to mark the retirement of Ian Speden* (pp. 7–11). Institute of Geological and Nuclear Sciences Science Report.

Isaac, M. J., Herzer, R., Brook, F. J., & Hayward, B. W. (1994). Cretaceous and cenozoic sedimentary basins of Northland. *New Zealand* (Vol. 8, p. 230). Institute of Geological & Nuclear Sciences monograph.

Jiao, R., Seward, D., Little, T. A., Herman, F., & Kohn, B. P. (2017). Constraining provenance, thickness and erosion of nappes using low-temperature thermochronology: The Northland allochthon, New Zealand. *Basin Research*, *29*(1), 81–95. https://doi.org/10.1111/bre.12166

Jones, J. G., & McDougall, I. (1973). Geological history of Norfolk and Philip Islands, southwest Pacific Ocean. *Journal of the Geological Society of Australia*, *20*(3), 239–254. https://doi.org/10.1080/14400957308527916

Juan, C., Collot, J., & Marcaillou, B. (2015). Rapport de traitement sismique post-campagne—Migration temps préstack Faust2, Rapport SGNC-2015.

Juan, C., Collot, J., & Marcaillou, B. (2016). Rapport de traitement sismique post-campagne—Migration temps préstack TECTA, Rapport SGNC-2016.

Karthikeyan, V., Collot, J., Etienne, S., Loubrieu, B., Patriat, M., Vendé-Leclerc, M., et al. (2022). Base de données de sondeurs multifaisceaux et modèles bathymétriques de la Nouvelle-Calédonie -hors lagon. *Rapport SGNC*, *2022*(12). https://doi.org/10.13155/91834

King, P. R., & Thrasher, G. P. (1996). *Cretaceous-Cenozoic geology and petroleum systems of the Taranaki Basin* (p. 243). Institute of Geological and Nuclear Sciences Limited, Lower Hutt.

Klingelhoefer, F., Lafoy, Y., Collot, J., Cosquer, E., Géli, L., Nouzé, H., & Vially, R. (2007). Crustal structure of the basin and ridge system west of New Caledonia (southwest Pacific) from wide-angle and reflection seismic data. *Journal of Geophysical Research*, *112*(B11102), B11102. https://doi.org/10.1029/2007jb005093

Lafoy, Y., Brodien, I., Vially, R., & Exon, N. F. (2005). Structure of the basin and ridge system west of New Caledonia (southwest Pacific): A synthesis. *Marine Geophysical Researches*, *26*(1), 37–50. https://doi.org/10.1007/s11001-005-5184-5

Lafoy, Y., van de Beuque, S., Missegue, F., Nercessian, A., & Bernadel, G. (1998). Campagne de sismique multitrace entre la marge Est Australienne et le Sud de l'arc des Nouvelles-Hébrides—Rapport de la campagne RIG SEISMIC 206 (21 avril—24 mai 1998)—Programme FAUSTRep (pp. 1–40).

Lagabrielle, Y., & Chauvet, A. (2008). The role of extensional faulting in shaping Cenozoic New Caledonia. *Bulletin de la Societe Geologique de France*, *179*(3), 315–329. https://doi.org/10.2113/gssgfbull.179.3.315

Lagabrielle, Y., Maurizot, P., Lafoy, Y., Cabioch, G., Pelletier, B., Régnier, M., et al. (2005). Post-Eocene extensional tectonics in Southern New Caledonia (SW Pacific): Insights from onshore fault analysis and offshore seismic data. *Tectonophysics*, *403*(1–4), 1–28. https://doi.org/10.1016/j.tecto.2005.02.014

Lallemand, S., & Arcay, D. (2021). Subduction initiation from the earliest stages to self-sustained subduction: Insights from the analysis of 70 Cenozoic sites. *Earth-Science Reviews*, *221*, 103779. https://doi.org/10.1016/j.earscirev.2021.103779

Lawrence, M. J. F., Morgans, H. E. G., Crundwell, M. P., & Patriat, M. (2019). Carbonate rocks of offshore northern Zealandia. *New Zealand Journal of Geology and Geophysics*, *63*, 1–24. https://doi.org/10.1080/00288306.2019.1626745

Leng, W., & Gurnis, M. (2015). Subduction initiation at relic arcs. *Geophysical Research Letters*, *42*(17), 7014–7021. https://doi.org/10.1002/2015GL064985

Matthews, K. J., Williams, S. E., Whittaker, J. M., Müller, R. D., Seton, M., & Clarke, G. L. (2015). Geologic and kinematic constraints on Late Cretaceous to mid Eocene plate boundaries in the southwest Pacific. *Earth-Science Reviews*, *140*(0), 72–107. https://doi.org/10.1016/j.earscirev.2014.10.008

Mauffret, A., Symonds, P. A., Meffre, S., Carson, L. J., & Bernardel, G. (2002). Geological and morphological framework of the Norfolk Ridge to three Kings Ridge region: The FAUST-2 survey area, *Geoscience Australia record* (pp. 2002–2008).

Maurizot, P. (2011). First sedimentary record of the pre-obduction convergence in New Caledonia: Formation of an early Eocene accretionary complex in the north of Grande Terre and emplacement of the "Montagnes Blanches" nappe. *Bulletin de la Société Géologique Française*, *182*(6), 479–491. https://doi.org/10.2113/gssgfbull.182.6.479

Maurizot, P. (2014). Evolution and sedimentation in a forebulge environment: Example of the late Eocene Uitoé limestone, New Caledonia, southwest Pacific. *New Zealand Journal of Geology and Geophysics*, *57*(4), 390–401. https://doi.org/10.1080/00288306.2014.938085

Maurizot, P., Bordenave, A., Cluzel, D., Collot, J., & Etienne, S. (2020). Late Cretaceous to Eocene cover: From rifting to convergence. *New Caledonia - Geology, geodynamic evolution, and mineral resources*, *51*(1), 53–91. https://doi.org/10.1144/M51-2017-18

Maurizot, P., Cabioch, G., Fournier, F., Leonide, P., Sebih, S., Rouillard, P., et al. (2016). Post-obduction carbonate system development in New Caledonia (Népoui, Lower Miocene). *Sedimentary Geology*, *331*, 42–62. https://doi.org/10.1016/j.sedgeo.2015.11.003

Maurizot, P., & Cluzel, D. (2014). Pre-obduction records of Eocene foreland basins in central New Caledonia: An appraisal from surface geology and Cadart-1 borehole data. *New Zealand Journal of Geology and Geophysics*, *57*(3), 1–12. https://doi.org/10.1080/00288306.2014.885065

Maurizot, P., Cluzel, D., Meffre, S., Campbell, H. J., Collot, J., & Sevin, B. (2020). Pre-Late Cretaceous basement terranes of the Gondwana active margin. In P. Maurizot & N. Mortimer (Eds.), *New Caledonia—Geology, geodynamic evolution, and mineral resources*. Geological Society, Memoirs.

Maurizot, P., Cluzel, D., Patriat, M., Collot, J., Iseppi, M., Lesimple, S., et al. (2020). The Eocene subduction-obduction complex of New Caledonia. In P. Maurizot & N. Mortimer (Eds.), *New Caledonia—Geology, geodynamic evolution, and mineral resources*. Geological Society, Memoirs.

Maurizot, P., & Mortimer, N. (Eds.) (2020). *New Caledonia: Geology, geodynamic evolution and mineral resources* (Vol. 51). Geological Society. https://doi.org/10.1144/M51

Maurizot, P., & Vendé-Leclerc, M. (2009). *Carte géologique de la Nouvelle-Calédonie, échelle 1/500 000 version 1*. Geological Survey of New Caledonia / BRGM.

McDougall, I., Hawkins, J. W., Parson, L., & Allan, J. (1994). Data report: Dating of rhyolitic glass in the Tonga forearc (Hole 841B). In *Proceedings of the ocean drilling Program*. Scientific Results.

Meffre, S., Crawford, A. J., & Quilty, P. G. (2006). Arc-continent collision forming a large island between New Caledonia and New Zealand in the Oligocene. In *Australian Earth sciences convention* (pp. 1–3).

Meffre, S., Falloon, T. J., Crawford, T. J., Hoernle, K., Hauff, F., Duncan, R. A., et al. (2012). Basalts erupted along the Tongan fore arc during subduction initiation: Evidence from geochronology of dredged rocks from the Tonga fore arc and trench. *Geochemistry, Geophysics, Geosystems*, *13*(12), Q12003. https://doi.org/10.1029/2012gc004335

Mitchum, R. H., Vail, P. R., & Thompson, S. (1977). Seismic stratigraphy and global changes of sea level. In C. E. Payton (Ed.), *Seismic stratigraphy—Application to hydrocarbon exploration* (Vol. 26, p. 516). AAPG Mem.

Monzier, M., & Vallot, J. (1983). Rapport préliminaire concerant les dragages réalisés lors de la campagne GEORSTOM III SUD (1975). *Office de la Rercherche Scientifique et Technique Outre-Mer, Centre de Nouméa, Geologie-Geophysique Rapport n°2-*, (Vol. 83, p. 77).

Mortimer, N. (2004). New Zealand's geological foundations. *Gondwana Research*, *7*(1), 262–272. https://doi.org/10.1016/s1342-937x(05)70324-5

Mortimer, N., Campbell, H., Tulloch, A. J., King, P. R., Stagpoole, V., Wood, R. A., et al. (2017). Zealandia: Earth's hidden continent. *Geological Society of America Today*, *27*(3), 27–35. https://doi.org/10.1130/GSATG321A.1

Mortimer, N., Herzer, R. H., Gans, P. B., Laporte-Magoni, C., Calvert, A. T., & Bosch, D. (2007). Oligocene-Miocene tectonic evolution of the South Fiji Basin and Northland Plateau, SW Pacific Ocean: Evidence from petrology and dating of dredged rocks. *Marine Geology*, *237*(1–2), 1–24. https://doi.org/10.1016/j.margeo.2006.10.033

Mortimer, N., Herzer, R. H., Gans, P. B., Parkinson, D. L., & Seward, D. (1998). Basement geology from three Kings Ridge to West Norfolk Ridge, southwest Pacific Ocean; evidence from petrology, geochemistry and isotopic dating of dredge samples. *Marine Geology*, *148*(3–4), 135–162. https://doi.org/10.1016/s0025-3227(98)00007-3

Mortimer, N., Patriat, M., Gans, P. B., Agranier, A., Chazot, G., Collot, J., et al. (2020). The Norfolk Ridge seamounts: Eocene–Miocene volcanoes near Zealandia's rifted continental margin. *Australian Journal of Earth Sciences*, *68*(3), 1–13. https://doi.org/10.1080/08120099.2020.1805007

Mortimer, N., Tulloch, A. J., & Ireland, T. R. (1997). Basement geology of Taranaki and Wanganui basins, New Zealand. *New Zealand Journal of Geology and Geophysics*, *40*(2), 223–236. https://doi.org/10.1080/00288306.1997.9514754

Nouzé, H., Cosquer, E., Collot, J., Foucher, J.-P., Klingelhoefer, F., Lafoy, Y., & Géli, L. (2009). Geophysical characterization of bottom simulating reflectors in the Fairway Basin (off New Caledonia, Southwest Pacific), based on high resolution seismic profiles and heat flow data. *Marine Geology*, *266*(1–4), 80–90. https://doi.org/10.1016/j.margeo.2009.07.014

O'Connor, J. M., Steinberger, B., Regelous, M., Koppers, A. A. P., Wijbrans, J. R., Haase, K. M., et al. (2013). Constraints on past plate and mantle motion from new ages for the Hawaiian-Emperor Seamount Chain. *Geochemistry, Geophysics, Geosystems*, *14*(10), 4564–4584. https://doi.org/10.1002/ggge.20267

Oke, P. R., Pilo, G. S., Ridgway, K., Kiss, A., & Rykova, T. (2019). A search for the Tasman front. *Journal of Marine Systems*, *199*, 103217. https://doi.org/10.1016/j.jmarsys.2019.103217

Orr, D., Sutherland, R., & Stratford, W. R. (2020). Eocene to Miocene subduction initiation recorded in stratigraphy of Reinga Basin, northwest New Zealand. *Tectonics*, *39*(2), e2019TC005899. https://doi.org/10.1029/2019tc005899

Paquette, J. L., & Cluzel, D. (2007). U-Pb zircon dating of post-obduction volcanic-arc granitoids and a granulite-facies xenolith from New Caledonia. Inference on Southwest Pacific geodynamic models. *International Journal of Earth Sciences*, *96*(4), 613–622. https://doi.org/10.1007/s00531-006-0127-1

Paris, J. P. (1977). *Carte Géologique à l'échelle du 1/50 000 et notice explicative: feuille Mouindou*. Territoire de la Nouvelle-Calédonie—Bureau de Recherches Géologiques et Minières.

Patriat, M., Collot, J., Etienne, S., Poli, S., Clerc, C., Mortimer, N., et al. (2018). New Caledonia obducted peridotite nappe: Offshore extent and implications for obduction and postobduction processes. *Tectonics*, *37*(4), 1077–1096. https://doi.org/10.1002/2017TC004722

Patriat, M., Mortimer, N., Agranier, A., Amann, M., Bassoulet, C., Campbell, H., et al. (2015). VESPA cruise, RV L'Atalante. https://doi.org/10.17600/15001100

Pirard, C., & Spandler, C. (2017). The zircon record of high-pressure metasedimentary rocks of New Caledonia: Implications for regional tectonics of the south-west Pacific. *Gondwana Research*, *46*, 79–94. https://doi.org/10.1016/j.gr.2017.03.001

Rait, G., Chanier, F., & Waters, D. W. (1991). Landward- and seaward-directed thrusting accompanying the onset of subduction beneath New Zealand. *Geology*, *19*(3), 230–233. https://doi.org/10.1130/0091-7613(1991)019<0230:lasdta>2.3.co;2

Rait, G. J. (2000). Thrust transport directions in the Northland Allochton, New Zealand. *New Zealand Journal of Geology and Geophysics*, *43*(2), 271–288. https://doi.org/10.1080/00288306.2000.9514886

Ravenne, C., De Broin, C. E., Dupont, J., Lapouille, A., & Launay, J. (1977). New Caledonia basin-Fairway ridge: Structural and sedimentary study. In *International symposium on geodynamics in the southwest Pacific* (pp. 145–154). Technip. Nouméa (New Caledonia).

Reagan, M. K., Ishizuka, O., Stern, R. J., Kelley, K. A., Ohara, Y., Blichert-Toft, J., et al. (2010). Fore-arc basalts and subduction initiation in the Izu-Bonin-Mariana system. *Geochemistry, Geophysics, Geosystems*, *11*(3), Q03X12. https://doi.org/10.1029/2009gc002871

Rouillard, P., Collot, J., Sutherland, R., Bache, F., Patriat, M., Etienne, S., & Maurizot, P. (2017). Seismic stratigraphy and paleogeographic evolution of Fairway Basin, northern Zealandia, southwest Pacific: From Cretaceous Gondwana breakup to Cenozoic Tonga–Kermadec subduction. *Basin Research*, *29*, 189–212. https://doi.org/10.1111/bre.12144

Schellart, W. P., Lister, G. S., & Toy, V. G. (2006). A Late Cretaceous and Cenozoic reconstruction of the Southwest Pacific region: Tectonics controlled by subduction and slab rollback processes. *Earth-Science Reviews*, *76*(3–4), 191–233. https://doi.org/10.1016/j.earscirev.2006.01.002

Sdrolias, M., Müller, R., & Gaina, C. (2003). Tectonic evolution of the southwest Pacific using constraints from backarc basins. *Geological Society of America Special Paper*, *372*, 343–359.

Secchiari, A., Montanini, A., Bosch, D., Macera, P., & Cluzel, D. (2018). The contrasting geochemical message from the New Caledonia gabbronorites: Insights on depletion and contamination processes of the sub-arc mantle in a nascent arc setting. *Contributions to Mineralogy and Petrology*, *173*(8), 66. https://doi.org/10.1007/s00410-018-1496-8

Sevin, B., Maurizot, P., Cluzel, D., Tournadour, E., Etienne, S., Folcher, N., et al. (2020). Post obduction evolution of New Caledonia. *New Caledonia—Geology, geodynamic evolution, and mineral resources* (Vol. 51, pp. 147–188). https://doi.org/10.1144/M51-2018-74

Shor, G. G., Kirk, H. K., & Menard, H. W. (1971). Crustal structure of the Melanesian area. *Journal of Geophysical Research*, *76*(11), 2562–2586. https://doi.org/10.1029/jb076i011p02562

Shuck, B., Van Avendonk, H., Gulick, S. P. S., Gurnis, M., Sutherland, R., Stock, J., et al. (2021). Strike-slip Enables subduction initiation beneath a failed rift: New seismic constraints from Puysegur margin, New Zealand. *Tectonics*, *40*(5), e2020TC006436. https://doi.org/10.1029/2020tc006436

Skinner, C., & Sutherland, R. (2022). Cretaceous rift-drift tectonics then Paleogene prearc subsidence related to subduction initiation: Aotea Basin, Zealandia, Southwest Pacific. *Tectonics*, *41*(1), e2021TC006820. https://doi.org/10.1029/2021tc006820

Smith, W. H. F., & Sandwell, D. T. (1997). Global Sea floor topography from satellite altimetry and Ship depth Soundings. *Science*, *277*(5334), 1956–1962. https://doi.org/10.1126/science.277.5334.1956

Spandler, C., & Hermann, J. (2006). High-pressure veins in eclogite from New Caledonia and their significance for fluid migration in subduction zones. *Lithos*, *89*(1–2), 135–153. https://doi.org/10.1016/j.lithos.2005.12.003

Spandler, C., Rubatto, D., & Hermann, J. (2005). Late Cretaceous-Tertiary tectonics of the southwest Pacific: Insight from U-Pb sensitive, high-resolution ion microphobe (SHRIMP) dating of eclogite facies from New Caledonia. *Tectonics*, *24*, TC3003. https://doi.org/10.1029/2004TC001709

Spörli, K. B., Aita, Y., & Gibson, G. W. (1989). Juxtaposition of Tethyan and non-Tethyan Mesozoic radiolarian faunas in melanges, Waipapa terrane, north island, New Zealand. *Geology*, *17*(8), 753–756. https://doi.org/10.1130/0091-7613(1989)017<0753:JOTANT>2.3.CO;2

Steinberger, B., Sutherland, R., & O'Connell, R. J. (2004). Prediction of Emperor-Hawaii seamount locations from a revised model of global plate motion and mantle flow. *Nature*, *430*(6996), 167–173. https://doi.org/10.1038/nature02660

Stern, R. J. (2004). Subduction initiation: Spontaneous and induced. *Earth and Planetary Science Letters*, *226*(3–4), 275–292. https://doi.org/10.1016/s0012-821x(04)00498-4

Stern, R. J., & Gerya, T. (2018). Subduction initiation in nature and models: A review. *Tectonophysics*, *746*, 173–198. https://doi.org/10.1016/j.tecto.2017.10.014

Stratford, W. R., Sutherland, R., & Collot, J. (2018). Physical properties and seismic-reflection interpretation of bathyal marine sediments affected by carbonate and silica diagenesis in the Tasman Sea. *New Zealand Journal of Geology and Geophysics*, *61*(1), 96–111. https://doi.org/10.1080/00288306.2017.1414065

Stratford, W. R., Sutherland, R., Dickens, G. R., Blum, P., Collot, J., Gurnis, M., et al. (2022). Timing of Eocene compressional plate failure during subduction initiation, northern Zealandia, southwestern Pacific. *Geophysical Journal International*, *229*(3), 1567–1585. https://doi.org/10.1093/gji/ggac016

Sutherland, R. (1999). Basement geology and tectonic development of the greater New Zealand region: An interpretation from regional magnetic data. *Tectonophysics*, *308*(3), 341–362. https://doi.org/10.1016/s0040-1951(99)00108-0

Sutherland, R., Collot, J., Bache, F., Henrys, S., Barker, D., Browne, G. H., et al. (2017). Widespread compression associated with Eocene Tonga-Kermadec subduction initiation. *Geology*, *45*(4), 355–358. https://doi.org/10.1130/G38617.1

Sutherland, R., Collot, J., Lafoy, Y., Logan, G. A., Hackney, R., Stagpoole, V., et al. (2010). Lithosphere delamination with foundering of lower crust and mantle caused permanent subsidence of New Caledonia trough and transient uplift of Lord Howe Rise during Eocene and Oligocene initiation of Tonga-Kermadec subduction, western Pacific. *Tectonics*, *29*(2), TC2004. https://doi.org/10.1029/2009tc002476

Sutherland, R., Dickens, G. R., Blum, P., Agnini, C., Alegret, L., Asatryan, G., et al. (2019b). Site U1508, proceedings of the international ocean discovery program; Tasman frontier subduction initiation and Paleogene climate; expedition 371 of the R/V JOIDES resolution (Vol. *371*, p. 44). *to Hobart, Australia; Sites U1506-U1511*.

Sutherland, R., Dickens, G. R., Blum, P., Agnini, C., Alegret, L., Asatryan, G., et al. (2020). Continental-scale geographic change across Zealandia during Paleogene subduction initiation. *Geology*, *48*(5), 419–424. https://doi.org/10.1130/g47008.1

Sutherland, R., Dickens, G. R., Blum, P., Agnini, C., Alegret, L., Asatryan, G., et al. (2019c). Site U1507, proceedings of the international ocean discovery program; Tasman frontier subduction initiation and Paleogene climate; expedition 371 of the R/V JOIDES resolution (Vol. *371*, p. 38). *to Hobart, Australia; Sites U1506-U1511*.

Sutherland, R., Dickens, G. R., Blum, P., Agnini, C., Alegret, L., Bhattacharya, J., et al. (2019a). Proceedings of the international ocean discovery program; Tasman frontier subduction initiation and Paleogene climate; expedition 371 of the R/V JOIDES resolution, Townsville, Australia, to Hobart, Australia; sites U1506-U1511. (Monograph).

Sutherland, R., Dos Santos, Z., Agnini, C., Alegret, L., Lam, A. R., Westerhold, T., et al. (2022). Neogene Mass Accumulation rate of carbonate sediment across northern Zealandia, Tasman Sea, southwest Pacific. *Paleoceanography and Paleoclimatology*, *37*(2), e2021PA004294. https://doi.org/10.1029/2021PA004294

Sutherland, R., Viskovic, P., Bache, F., Stagpoole, V., Collot, J., Rouillard, P., et al. (2012). *Compilation of seismic reflection data from the Tasman Frontier region, southwest Pacific*. (p. 57). GNS Science Report.

Tapster, S., Roberts, N. M. W., Petterson, M. G., Saunders, A. D., & Naden, J. (2014). From continent to intra-oceanic arc: Zircon xenocrysts record the crustal evolution of the Solomon island arc. *Geology*, *42*(12), 1087–1090. https://doi.org/10.1130/G36033.1

Tournadour, E., Fournier, F., Etienne, S., Collot, J., Maurizot, P., Patriat, M., et al. (2020). Seagrass-related carbonate ramp development at the front of a fan delta (Burdigalian, New Caledonia): Insights into mixed carbonate-siliciclastic environments. *Marine and Petroleum Geology*, *121*, 104581. https://doi.org/10.1016/j.marpetgeo.2020.104581

Ulrich, M., Picard, C., Guillot, S., Chauvel, C., Cluzel, D., & Meffre, S. (2010). Multiple melting stages and refertilization as indicators for ridge to subduction formation: The New Caledonia ophiolite. *Lithos*, *115*(1), 223–236. https://doi.org/10.1016/j.lithos.2009.12.011

Vitale Brovarone, A., Agard, P., Monié, P., Chauvet, A., & Rabaute, A. (2018). Tectonic and metamorphic architecture of the HP belt of New Caledonia. *Earth-Science Reviews*, *178*, 48–67. https://doi.org/10.1016/j.earscirev.2018.01.006

Whattam, S., Malpas, J., Ali, J. R., Lo, C. H., & Smith, I. E. M. (2005). Formation and emplacement of the Northland ophiolite, northern New Zealand: SW Pacific tectonic implications. *Journal of the Geological Society of London*, *162*(2), 225–241. https://doi.org/10.1144/0016-764903-167

Whattam, S. A. (2009). Arc-continent collisional orogenesis in the SW Pacific and the nature, source and correlation of emplaced ophiolitic nappe components. *Lithos*, *113*(1–2), 88–114. https://doi.org/10.1016/j.lithos.2008.11.009